Preparation of Synthetic 'As-Damaged' Models for Post-earthquake BIM Reconstruction Research

Ling Ma[1], Rafael Sacks[2], Reem Zeibak-Shini[3], Ashrant Aryal[4] and Sagi Filin[5]

Abstract: Post-earthquake operations, such as search and rescue and damage assessment, require efficient and effective surveying technologies to rapidly capture the 'as-damaged' state of buildings. Recent research has shown early feasibility of methods for compilation of 'as-damaged' building information models (BIM) from

---

[1] Postdoctoral Researcher, Virtual Construction Laboratory, National Building Research Institute, Technion – Israel Institute of Technology, Haifa 32000, Israel +972-4-8292245, lingma@technion.ac.il

[2] Assoc. Prof., Head Dept. of Structural Engineering and Construction Management, Faculty of Civil and Env. Eng., Technion – Israel Institute of Technology, Haifa 32000, Israel +972-4-8293190, cvsacks@technion.ac.il

[3] PhD Candidate, Virtual Construction Laboratory, National Building Research Institute, Technion – Israel Institute of Technology, Haifa 32000, Israel +972-4-8293120, reemz@technion.ac.il

[4] Undergraduate Research Assistant, Virtual Construction Laboratory, National Building Research Institute, Technion – Israel Institute of Technology, Haifa 32000, Israel +972-4-8293120, aryal@t2.technion.ac.il

[5] Assoc. Prof., Head Dept. of Transport Engineering and Geo-Informatics, Faculty of Civil and Env. Eng., Technion – Israel Institute of Technology, Haifa 32000, Israel +972-4-8295855, filin@technion.ac.il

'as-damaged' point cloud data and ‘as-built’ models. Yet research efforts to develop and rigorously test appropriate methods are seriously hampered by the obvious scarcity of access for researchers to earthquake-damaged buildings for surveying specimens and hence the lack of terrestrial laser scanning data of post-earthquake buildings. Full- or reduced-scale physical models of building components can be built and damaged using a shaking table or other structural laboratory equipment, and these can be scanned, all at reasonable cost. However, equivalent full-scale building samples are unavailable. The solution is to synthesize accurate and representative data sets. A computational approach for compiling such data sets, including BIM modeling of damaged buildings and synthetic scan generation, is proposed. The approach was validated experimentally through compilation of two full-scale models of buildings damaged in earthquakes in Turkey.

Author keywords: Building Information Modeling; Earthquake damage; Damaged building; Experimental dataset; Laser scanning emulator; Synthetic point clouds.

Subject headings: Building Information Modeling; Damage; Earthquake; Surveys.

1 Introduction

In the Search and Rescue (S&R) phase after an earthquake, rescue teams require detailed information about the location and shape of voids in buildings where survivors may be trapped and any possible pathways to reach them (Tiedemann 1992). For the subsequent Reconstruction & Recovery (R&R) phase, inspectors need information about the deformation and displacement that building components have sustained in order to assess the damage.

The Federal Emergency Management Agency guide to earthquake damage assessment, FEMA 306 (1998) details what information should be collected and how it should be documented in a survey process. However, the conventional procedure is laborious and time-consuming. A more efficient and effective survey technology is needed, especially given the emergent and hazardous environment. The need arises to rapidly and safely gather information regarding the geometry and placement of damaged building components.

At the level of detail of the structure as a whole, airborne laser scanning technology has been applied in post-earthquake responses for identification of damaged buildings (P. L. Dong and Guo 2012; Liu et al. 2013) and for classification of the buildings according to the type of damage sustained (L. G. Dong and Shan 2013). However, in the use case of S&R and R&R, higher resolution is required for identifying damage at the level of detail of individual building components, and this cannot be achieved with airborne laser scanning.

Terrestrial laser scanning (TLS) and 3D photogrammetry can provide high-resolution 3D point clouds from convenient locations near to a damaged building. TLS has been tested with fairly good results for the case of buildings damaged in a tornado (Kashani et al. 2014), although the procedure did not extend as far as reconstructing BIM models of the post-disaster structures. Using videogrammetry rather than laser scanning, German et al. (2013) developed an approach based on real-time analysis of video frames to identify the cracks in concrete columns and other structural elements. Torok et al. (2014) proposed an unmanned robotic platform equipped with 3D camera to identify cracks on structural elements.

In these examples, the goal is restricted to identifying damage but not to reconstructing models. Therefore, in an attempt to meet the need for reconstructed BIM models that provide detailed information about a damaged building, including the geometry and semantics of interior elements and voids, a team at the Technion engaged in research to develop a system that can reconstruct an 'as-damaged' BIM model on the basis of an ‘as-built’ model and point cloud data describing the post-earthquake condition of the building (Zeibak-Shini, Sacks, and Filin 2012; Bloch 2014). However, this effort was severely restricted by the lack of available point cloud data and specimens of buildings that have suffered earthquake damage. Unlike the case of airborne and space-based imagery, where extensive datasets are provided online by various government agencies and NGOs after earthquake events, such as OpenTopography (Krishnan et al. 2011), no similar TLS datasets are available.

To overcome this problem, we have developed a computational approach to synthesize accurate and representative data sets that include ‘as-built’ BIM models, terrestrial laser scan point cloud data, and 'as-damaged' building models that can be used for rigorous testing of the above-mentioned methods. The following section describes the workflow of the research and development (R&D) of the overall 'Scan-to-BIM' system, highlighting the challenges faced due to the lack of 'as-damaged' data for experimentation. In section 3 and 4, two methods for preparing 'as-damaged' models are compared. Section 0 presents two full-scale cases where 'as-damaged' scans and models are produced using the proposed approach, and section 6 describes validation of the synthetic scans from one case by application of the first step of the 'Scan-to-BIM' process.

2 Workflow and Challenges in the Earthquake 'Scan-to-BIM' R&D

The first prerequisite for the R&D is to prepare an 'as-damaged' model for testing and validating the 'Scan-to-BIM' system. For obvious reasons, the experimental research cannot be performed 'in-situ' within the context of a real earthquake. Seismic response research therefore relies on earthquake shaking tables or computer simulations.

Building a large-scale shaking table for physical earthquake experiments (Kasai et al. 2010; van de Lindt et al. 2010; Panagiotou, Restrepo, and Conte 2010) takes many years and requires very large investments. For example, the world's largest shaking table, E-defense (Ohtani et al. 2003), took 5 years to build; building the large high performance outdoor shaking table (LHPOST) (Conte et al. 2004) cost $5.9 million. Most researchers cannot afford such full-scale seismic damage simulation platforms. Thus a more practical approach for preparing damaged specimens is needed.

The second prerequisite is to scan specimens using LiDAR (Light Detection and Ranging) equipment. In order to obtain a panoramic view of the complete model, several aspects of the target structure should be scanned. The multiple scans from different viewpoints can be combined into one scene in the same global reference frame (termed registration) as a function of the placements of the scanner and the layout of auxiliary targets (Becerik-Gerber et al. 2011). In addition, the accuracy of the acquired point cloud is affected by the noise and outlier background data (Eo et al. 2012). Much research has focused on the data pre-processing problems, which can be minimized by the use of laser scanners with a) geo-referencing capability, such as highly accurate GPS, so that registration of multiple scans could be easily performed (Previtali et al. 2014); and b) with flexible control on the point cloud properties, such as accuracy of point position and distance, precision of modelled surface against noise, spot size, point spacing (Lichti, Gordon, and Tipdecho 2005) etc.

Together with the captured 'as-damaged' state of the specimen, the 'as-built' state of the building is also required for change detection. The geometry, the material, component classification and other semantic information are all required in damage assessment. Given that BIM is a well-accepted technology for modeling 'as-built' and 'as-designed' states of a building (Eastman et al. 2011), an 'as-built' BIM model is compiled in the process of the experimental research.

3 Preparation of Real Models and Scans

Confronted with the challenges described above, we tested two approaches to prepare 'as-damaged' models and scans. The first approach used real full-scale specimens, albeit not of whole buildings, but rather individual building elements and small frames. The second approach was computational, using BIM software and a custom-built laser scanner emulator to compile synthetic point clouds of 'as-damaged' building models. This section of the paper describes the former approach, and section 4 describes the latter.

3.1 Preparing Experimental Specimens

The damaged specimens resulted from earlier research in the structures laboratory at the National Building Research Institute (NBRI) at the Technion in which seismic loads were applied to simple reinforced concrete beams and frames. Two available specimens were selected for experimentation. One is a reinforced concrete beam and the other is a reinforced concrete frame wall with autoclaved cement block infill. Both specimens had sustained some damage. As shown in Fig. 1, the beam was mainly damaged by bending, whereas the frame sustained cracks, shearing and bending in the infill, beams and columns respectively (Schwarz, Hanaor, and Yankelevsky 2008).

Fig. 1. Reinforced concrete specimens tested at NBRI: (a) a damaged reinforced concrete beam and (b) a damaged reinforced concrete frame wall with autoclaved cement block infill.

3.2 Modeling the 'As-Built' BIM Model of the Specimen

In order to provide the ‘as-built’ information, BIM models of the undamaged beam and frame were compiled based on the shop drawings, as is shown in Fig. 2. The reinforced concrete frame wall was composed of basic elements: columns, beams and a panel. Following damage, changes occur to those elements, their state, form, location, and connections to their neighbors.

Fig. 2. Preparation of as-built BIM model: (a) 2D drawing of the reinforced concrete beam; (b) 2D drawings of the reinforced concrete frame; (c) 'As-built' BIM model of the beam; (d) 'As-built' BIM model of the frame

3.3 Field scanning of damaged structures

A Leica ScanStation C10 (2014) was used to perform the field scanning. The scan rate is up to 50,000 points/sec. The accuracy of a single range measurement is ±4mm in range and ±6mm in position. The scanning field of view is 360º horizontally and 270º vertically. Scanning a specific and small structure using the 360º scanning application is inefficient. Instead, a more efficient and time saving technique is used where the structure is targeted using the scanner's camera and a scanning window is defined with maximum and minimum scanning angles in both directions (vertical and horizontal). Such a scan takes only a few minutes. The acquired point clouds are shown in Fig. 3.

Fig. 3. Point clouds of (a) the beam and (b) the wall frame.

The major challenge in preparation of real experimental specimens and scans is that the majority of researchers cannot afford facilities for full-scale earthquake simulations. Furthermore, experiments carried out on the simple damaged specimens are fairly limited and cannot guarantee that a 'scan-to-BIM' protocol would provide reliable results when applied to more complicated full-scale cases.

4 Preparation of Synthetic Models and Scans

Given the challenges in preparing 'as-damaged' models and scans of real specimens and buildings, we propose a new computational procedure to provide synthetic 'as-damaged' models and scans. The workflow of the procedure is shown in Fig. 4 within the context of the overall earthquake 'Scan-to-BIM' system. The system includes four kernel parts: a BIM handler for preparing the 'as-built' and 'as-damaged' BIM models that serve as specimens in the experiments; a laser scanning emulator to produce synthetic point cloud data of the same quality as would result from laser scanning in the field; a point cloud processing step in which algorithms are developed for automatic or semi-automatic compilation of the semantic 'as-damaged' BIM model; and a model checking step to test the effectiveness of the processor by comparing the two 'as-damaged' BIM models that are produced in steps one and three respectively. Steps one and two are the subjects of this paper.

Fig. 4. BIM Modeling and Scan emulation steps (1 and 2) within the context of the broad earthquake 'Scan-to-BIM' research process

4.1 Modeling of Synthetic Damage

The 'as-built' BIM model is the first prerequisite in the procedure. This is straightforward to prepare, based on the building’s design and construction drawings.

The next step is to compile a BIM model for the 'as-damaged' state of the building using the same modeling approach. The authors (Ma, Sacks, and Zeibak-Shini 2014) have proposed an extension to the IFC schema (BuildingSmart 2013) which lays the groundwork for BIM modeling of the damaged building components. The IFC-based data schema has the advantage that all the semantic information that describes building components, including their identity, classification, material, etc., is well defined. The extended part of the schema associates the 'as-built' BIM model with the 'as-damaged' model in a single exchange file and maintains a record of the progressive damage process in the file.

Pending eventual adoption of the proposed schema extensions, standard objects within commercial BIM tools can be used to model the damaged components, using existing Boolean solid modeling functions. In this strategy, typical earthquake damage modes of reinforced concrete building components (such as spalling, delamination, bending and buckling, breaking, etc.) can generally be represented by using successive solid clipping operations to mimic the progress of structural damage in reinforced concrete components. With this approach, one can model the damaged components in most commercial BIM software. The modeling approach is described in the following paragraphs.

In BIM tools with solid modeling, the damaged objects can be built by clipping the original ‘as-built’ objects with void components. The sharpness of the cracked segment can be adjusted by manipulating the dimensions, location and orientation of the void component, as is shown in Fig. 5. In other tools, the solid modeling is implemented using functions such as ‘cut part with another part’. The cutting part can be moved and rotated very precisely to the desired location and orientation. The cutting part can then be deleted after the operation, leaving behind the void geometry.

Fig. 5. Modeling of damaged building components in BIM tools

One drawback of modeling the damaged building with these software tools is that when creating damaged building components, each damaged segment is treated as a new building component, so that the resulting segments are unrelated to the original building components to which they correspond. The aggregation relationships between the damaged segments and the original building components from which they were derived are not modeled.

A second issue arises in BIM applications in which the functional classification of a building component is dependent on its orientation in space. In Tekla Structures, for example, a column is classified at run-time as a longitudinal element whose top point lies directly above its bottom point. If a column is rotated away from the vertical within the process of modeling its ‘as-damaged’ state, it is automatically reclassified as a brace or a beam.

In order to fix these problems, we developed a software tool to edit the IFC file exported from the BIM application software to correct the component type and to add the aggregation relationship between the original model components and the components of the damaged model. An example is illustrated in the following paragraphs.

Fig. 6. The ‘as-damaged’ frame modeled in Revit.

First, the 'as-built'/'as-designed' BIM model (Fig. 2(d)) is compiled in Revit and an IFC file of the model is exported. The GUID (Globally Unique Identifier) of each original building component can be acquired from the IFC file. Next, by examining the damage on site from photographs (Fig. 1(b)), the damaged building is also modeled in Revit (Fig. 6). The body clipping operation automatically replaces the original building components with new distinct building components, which represent the damage resulting segments in geometry but have no relationship in semantics. As is shown in **Fig. 7** (a), after clipping twice, the top beam becomes three distinct beams in Revit, although it would be semantically correct if it were represented as one damaged beam with three parts.

In order to correct this semantic problem and maintain the connection between ‘as-built’ and ‘as-damaged’ models, the GUID of the original component, which was acquired from the IFC file of the ‘as-built’ model, is entered into the ‘object type’ property of each of the corresponding new components in the ‘as-damaged’ Revit model. The ‘as-damaged’ model is then exported to an IFC file. The ‘post-processor’ editing tool parses the IFC file, identifies components with the same ‘object type’ properties, extracts their shape representations, and assembles these sets of shapes into single components in a new IFC file. In this new 'as-damaged' file all the components have 1:1 correspondence with the original components, they have the same GUID value, and they inherent all other semantic information from them. As shown in **Fig. 7** (b), the three parts of the upper beam are assembled as one damaged beam component. The IFC ‘post-processor’ tool was developed using IfcOpenShell (2014), a 3rd party c++ library.

Fig. 7. Enrichment of the 'as-damaged' model: (a) 'As-damaged' model built in Revit; (b) Aggregated geometry resulting from the custom-built post-processor

4.2 Laser scanning emulator

Another benefit of modeling synthetic 'as-damaged' BIM models is that digital building models can be 'scanned' by a tailored emulator to generate synthetic point cloud data by mimicking the mechanism of laser scanning in the field.

Ip and Gupta (2007) proposed a method to generate synthetic point clouds by directly sampling points on visible surface primitives of a 3D CAD model. However, they did not consider the fact that object surfaces are often partially or wholly occluded, where the point sampling method will fail to give the right result. Bosche et al. (2009) proposed a method to mimic the scanning process by transmitting virtual laser beams to 'hit' the 3D CAD model. The generated synthetic point cloud data is accurate and object occlusion is considered.

In this work, we build on Bosche et al. (2009)’s method but improve it in two ways. First, their scanning process extracts triangular meshes from the 3D CAD model, which results in very large data sets if the building model is composed of a number of polyhedron objects. We merged all the connected and coplanar triangular meshes into one single planar polygon, which decreases the number of meshes, thus significantly reducing the computation complexity. Second, not all the faces of a 3D object are visible in one scan. A cuboid, for example, has three faces at most that are visible in any one scan. We filter out all the invisible faces before executing the scanning process, which also reduces the number of primitives that needs to be handled, consequently further reducing the computational complexity. These two computational improvements are important because, when applying the synthetic scan to a large scale building structure with high scanning resolution, millions of 3D points are generated and this can take quite a long time.

Fig. 8. Workflow of the laser scanning emulator

The detailed workflow of the proposed laser scanning emulator is shown in **Fig. 8**. The editing tool built using IfcOpenShell (2014) is used to parse the IFC file and another tool, implemented using the Open CASCADE (2014) 3rd party c++ library, is applied to convert the arbitrary shape representations of the building elements in the IFC file to faceted boundary representation. This converts the BIM model to a set of 3D planar polygons that are encoded with the GUID of building components. Next, the user picks a suitable viewport as the placement of the virtual scanner. If the angle between the normal direction (pointing outwards) of a target facet and the inverse scanning direction (from the centroid of the target facet to the scanner) is greater than 90 degrees, then this facet is classified as an invisible facet in advance. Only visible facets are used to perform the scan.

Next, the emulator 'transmits' virtual laser beams in all directions at uniformly spaced angle intervals, as shown in Fig. **9**. For each transmitted laser beam, all the potential intersected facets are traversed to compute the line-plane intersections. Only the closest intersection is added to the synthetic point cloud: others are occluded in the model. The range of the virtual scanner to the intersection point of a particular laser beam, *r*, is defined as follows:

$$r = -d / (N^T \cdot \begin{bmatrix} \cos\varphi\cos\theta & \sin\theta & \sin\varphi\cos\theta \end{bmatrix}^T) \quad (1)$$

Fig. 9. The emulator 'transmits' virtual laser beams

where N is the normal vector of the intersected facet, d is the scalar coefficient of the intersected facet, θ and φ are the tilt and pan angle of the laser beam. Consequently, according to the transformation from spherical coordinates system to Euclidean coordinates system, the coordinates of the intersected point are derived as follows:

$$\begin{bmatrix} x \\ y \\ z \end{bmatrix} = r \begin{bmatrix} \cos\varphi\cos\theta \\ \sin\theta \\ \sin\varphi\cos\theta \end{bmatrix} \quad (2)$$

Each facet of 3D solid is (or approximates) a bounded plane surface, i.e., a planar polygon. For a specific polygon, there's no need to traverse the laser beam in all directions to 'hit' it. As a result, for each facet, the scope of pan and tilt angle in which the transmitted laser beams may potentially intersect with objects of interest is pre-calculated in the following way. First, the pan and tilt angles of the laser beams that reach the vertices of the facet are calculated. Then, the corresponding min-max pan and tilt angles among them are taken as the angle boundary of the target facet. Given that all the visible facets are labeled with boundaries defined as angles, for a specific transmitted laser beam, only the facets whose angle boundary covers the pan and tilt angle of the laser beam are selected to locate the line-plane intersection. Note that a consecutive set of laser beams that are included in an angle boundary form a spherical wedge, as is shown in Fig. 10. However, no planar polygon that is included in the spherical wedge can cover all the laser beams in the wedge. As a result, there must be some line-plane intersections that are not included in the planar polygon on the same plane. In other words, the laser beams included in the wedge may reach some area outside the contour of the planar polygon, but still on the polygon's plane. In this case, the line-plane intersection located by Eq. (1) will be a fake point in the point clouds. In order to filter out those outliers, we developed a program to test whether a point is included in a 3D polygon by extending PNPOLY (2014), which works only for the case of 2D polygons.

Fig. 10. Pan and tilt angle boundary

The synthetic point clouds generated by the above algorithm have perfect accuracy, unlike real scans, which are subject to inaccurate measurement. There are different sources of inaccuracy in laser-scanned point cloud data (Boehler, Bordas Vicent, and Marbs 2003), including both scanner induced inaccuracy (due to hardware and software effects) and optical effects associated with the target (occlusions and non-reflective surfaces).

Range and position measurement inaccuracy can be introduced into the synthetic point cloud by adding noise (Gaussian distributed random numbers) to Eq.(1) and Eq.(2) respectively. The magnitude of noise/inaccuracy can be controlled by manipulating the standard deviation of a random number generator. Gaussian noise widely exists in signal, image, video, etc., particularly when the sources of error are independent. Although some sources of noise in scanning have been found to exhibit some correlation (Sun et al. 2008), the resulting error in the inaccuracies ascribed to the range differences by using Gaussian distribution are far smaller than the tolerances used in the segmentation of the point clouds. As a result, Gaussian noise is chosen for representing the range and position inaccuracy.

Occlusions can also be introduced into the synthetic point cloud by placing 'cluttering' model objects (e.g., trees, utility poles) in the field of view of the scanner as part of the BIM model. Non-reflective surfaces are emulated simply by removing any objects, such as those made of glass, from the BIM model. Glass window panes thus appear as voids in the point cloud, just as they do in the real world (Pu and

Vosselman 2007).

Thus the operator/researcher has flexible control over the accuracy of point clouds for different purposes. For example, when the objective of the experiment is to validate the algorithm, the emulator can generate perfectly accurate data for testing, when the objective is to develop a robust system, the emulator can generate noisy data in a manner similar to the field scan. In addition, by manipulating the placement of the virtual scanner, new synthetic point clouds can be generated in minutes. Since the model is referenced in the coordinate system of the emulator, multiple scans are naturally matched, so that a ‘panorama’ of the model can be easily compiled and no registration work is needed.

5 Full-scale Case Studies

The EERI online repository (2014a) contains many data sets of buildings damaged in earthquake events. The data includes 2D drawings of the damaged buildings, photos of the pre- and post-event state of the buildings, etc. Two cases were selected in which the drawings and photos contained sufficiently clear and detailed information to allow understanding and modeling of the geometry of the building before and after the earthquake.

The 'as-built' BIM models were prepared based on the 2D drawings and photos of the original buildings, using both Autodesk Revit 2014 and Tekla Structures v20.0 software. The 'as-damaged' models were prepared based on the ‘as-built’ models and by examining the site photos of the damaged buildings. For these cases, only the structural frames and the masonry infill walls were modeled. Other components such as doors and windows were not included in the models. Finally, the custom-built scanner emulation software generated the synthetic point cloud data using the ‘as-damaged’ models.

The synthetic scanning process was performed in a manner similar to the way in which the field scanning process would have been performed in the real post-earthquake response. The scanning positions must be 'possible' in that they must be performed from locations in which it is physically possible to place a scanner in the field. To ensure this condition, viewpoints were chosen that corresponded to the viewpoints of the various photographs available in the EERI database. The density of the laser beams is adjustable by the user; different densities result in different resolutions of the point cloud. Each scan took some minutes, depending on the resolution selected.

5.1 Case 1

In the 2003 Bingol Earthquake, Turkey, magnitude 6.4, a school was damaged in the city of Kaleonu. The building was built in 1999 and had a reinforced concrete moment resisting frame. The typical column dimension was 300mm × 500mm and the typical beam dimension was 300mm × 700mm. The infill walls were made of hollow clay-tile masonry units with typical thickness of 250mm for internal walls and 400mm for external walls. The information regarding this building before and after the earthquake was obtained from the website of EERI (2014b). A photograph of the damaged building is shown in Fig. 11 (a). This building sustained heavy damage including a pancake collapse of the ground floor. The walls were partially delaminated and partially broken from the structure. The columns were broken and displaced from their original position. Slabs and beams sustained bending and were broken at several locations.

The ‘as-built’ and the 'as-damaged' BIM models are compared in Fig. 11 (c) and (d). Both were built in Tekla Structures v20.0. Some of the typical damaged components are listed in Table 1. The synthetic point cloud data was generated using our custom-built emulator software, and are shown in Fig. 11 (b).

Fig. 11. Preparation of the 'as-damaged' model for the damaged school: (a) Photograph showing earthquake damage to the school (EERI 2014b); (b) synthetic point clouds of the external facades of the damaged school; (c) as-built model of the school; (d) 'as-damaged' model of the school

Table 1. Typical damaged components in the school.

Building Component (numbering according to the notation in Fig. 11)	Component Type	Damage Description
1	Column	Portions missing, the remaining part is rotated
2	Column	Split into two distinct parts, both are rotated with small lateral deformation
3	Beam	Rotated and downward displaced of

		almost one floor
4	Beam	Broken into two distinct parts with downward displacement of almost one floor,
5	Masonry wall	Portions missing, blocks fallen out

5.2 Case 2

In the Kocaeli earthquake, Turkey, magnitude 7.6, August 17th 1999, a six-story residential building was damaged. The building was approximately 18.0m high, 19.4m wide and 23.2 m long. The structural system consisted of reinforced concrete moment frames in both directions and the floor system was an "Asmolen" slab (ribbed slab) with a typical thickness of 300mm (200 mm block and 100 mm slab). Asmolen slab systems are composed of one-way joists that are formed by hollow clay tile blocks; the slab between the joists is cast directly atop the blocks. The infill walls were made of hollow clay-tile masonry units. Both the 'as-built' and 'as-damaged' models for this building were compiled from information available on the website of EERI (EERI 2014c). A photograph of the damaged building is shown in Fig. 12 (a). This building had sustained severe damage. In general, the slabs were bent; most of the walls had fallen off, while the columns were almost in their original positions.

The 'as-built' model and the 'as-damaged' model are compared in Fig. 12 (c) and (d). Some of the typical damaged components are listed in Table 2. The point cloud generated in the emulator is shown in Fig. 12 (b).

Fig. 12. Preparation of the 'as-damaged' model for the residential building: (a) Photograph showing earthquake damage to the building (EERI 2014c); (b) synthetic point clouds of the external facades of the building; (c) 'as-built' model of the building; (d) 'as-damaged' model of the building

Table 2. Typical damaged components in the damaged residential builidng

Building Component (numbering according to the notation in Fig. 12)	Component Type	Damage Description
1	Wall	Completely detached from the structure and fallen off
2	Slab	Bent into two distinct parts
3	Wall	Displaced coherently with the deformation of the slab

5.3 Summary of results

In comparison with the costs of experiments with full-scale or even small-scale physical building models, the proposed procedure for preparing BIM models of an ‘as-built’ and the 'as-damaged' building is highly efficient. An undergraduate student with just one-year experience operating a BIM application can prepare the models without difficulty within short times. The durations spent on modeling the two cases are shown in Table 3. In addition, the synthetic point cloud data generated by the laser scanning emulator is of good quality, and the scanning process is quite efficient, as is shown in Table 3. Note that only the external facades were selected for scanning in the first case, while the whole model was scanned in the second case, so the scanning process for the second case took significantly longer time. However, preparation of the 'as-damaged' model of the second case took less time, because the damage modes of the structure were simpler. The emulator was running on a PC with an Intel Core i7-4770 CPU @ 3.4GHz and 8GB of RAM.

Table 3. Specification of the modeling process in case study

Tasks or parameters	School building	Residential building
Modeling tasks		
Preparing the 'as-built' BIM model based on drawings and photos	5 hours	8 hours
Modeling the damaged building based on 'as-built' model and photos	15 hours	10 hours
Refining the 'as-damaged' BIM model by aggregating the related damaged segments into objects using custom-built software	< 1 minute	< 1 minute
Laser scanning emulator data		
Angular spacing	0.02 degree	0.02 degree
Point spacing	15 mm	24 mm
Processing time	12min 40sec	21min 40sec

6 Validation of suitability for 'Scan-to-BIM' R&D

The original motivation for this work was to develop a versatile experimental setup to provide specimens for earthquake 'Scan-to-BIM' research. To validate the resulting point clouds, we compare execution of the initial steps of the overall ‘Scan-to-BIM’ system on the products of the synthetic process with execution of the same steps on real point cloud data.

The first step in the system is planar segment extraction. The segmentation algorithm was first applied to the point cloud data of the physical frame specimen mentioned above in **Fig. 3** (b). The segmentation result is shown in **Fig. 13** (a). As can be clearly seen, the right side column buckled and has divided into two distinct solid parts; the top beam bent and divided into three parts, and some bricks in the masonry wall were shifted or cracked.

Next, the same algorithm was applied to the synthetic point cloud generated in the first case study, shown in **Fig. 11** (b). The result is shown in **Fig. 13** (b). Here too, the identified planar segments clearly reflect the general geometrical features of the damaged state of the building façade, as can be seen by examining the photograph in **Fig. 11** (a). Note that windows appear as voids in the segmentation result, because they were not modeled in the synthetic 'as-damaged' BIM model.

Fig. 13. Segmentation results of (a) the physical specimen and (b) the synthetic specimen from case study 1. The colors code for normal vector values.

The real and the synthetic segmentation results are equivalent in terms of their data structure, their resolution and their representation of the damaged components. Differences in content occur only as a function of the content included or excluded through the BIM modeler's choices when compiling the 'as-damaged' BIM model, and not as a result of the function of the emulator software. As such, the modeler has full control of the output and the synthetic point cloud data are an effective substitute for the real point cloud data.

7 Conclusion

TLS is an emerging surveying technology and a promising solution for damage inspection in post-earthquake responses, and indeed for as-built or damage inspection in other, more common situations. Yet research efforts to develop these capabilities have been hampered by scarcity of access to the field to collect data from buildings that have suffered real earthquake damage and the costs of preparing physical specimens of damaged buildings or their components.

A computational approach is proposed to compile synthetic 'as-damaged' BIM models and a versatile laser scanning emulator has been developed to generate synthetic point cloud data in a manner similar to laser scanning on site. In addition, the procedure and the experimental setup provide an ideal benchmark (the user prepared 'as-damaged' model) for validating the system-generated 'as-damaged' model for research and development of a ‘Scan-to-BIM’ system. Implementation of the approach for two full-scale case studies has provided models and point cloud data. Application of the segmentation algorithm to the real and to the synthetic point cloud data produced equivalent and syntactically and semantically indistinguishable results from both, showing that the experimental setup can indeed serve as a substitute for physical specimens or for in-situ scans of earthquake-damaged buildings.

Future work will implement the above-mentioned computational method to pool a data repository of 'as-damaged' data models; including BIM model and synthetic scan, of real earthquake events. In addition, other applications of TLS in construction, such as automated quality control (Akinci et al. 2006) and construction progress control (Zhang and Arditi 2013), can also benefit from using the proposed method to prepare synthetic specimens. For example, researchers can generate point cloud data representing defects or damage to a building, or representing intermediate construction stages of a building, by modifying the placement, shape representation and visibility of the building components in BIM models. Thus we envision that the experimental setup could stimulate research in these emerging fields and promote the maturity of the technology.

8 Acknowledgment

This research was funded in part by the Insurance Companies Association of Israel. Dr. Ma is supported in part at the Technion by a fellowship from the Israel Council for Higher Education. The assistance of undergraduate research assistant Zhaoxin Fu is greatly appreciated.

9 References

Akinci, B., F. Boukamp, C. Gordon, D. Huber, C. Lyons, and K. Park. 2006. "A Formalism for Utilization of Sensor Systems and Integrated Project Models for Active Construction Quality Control." *Automation in Construction* 15 (2): 124–38.

Becerik-Gerber, Burcin, Farrokh Jazizadeh, Geoffrey Kavulya, and Gulben Calis. 2011. "Assessment of Target Types and Layouts in 3D Laser Scanning for Registration Accuracy." *Automation in Construction* 20 (5): 649–58.

Bloch, Tatyana. 2014. "Towards Building Information Modeling of Damaged Buildings to Guide Search and Rescue Operations." Technion. http://www.graduate.technion.ac.il/Theses/Abstracts.asp?Id=28075.

Boehler, Wolfgang, M. Bordas Vicent, and Andreas Marbs. 2003. "Investigating Laser Scanner Accuracy." *The International Archives of Photogrammetry, Remote Sensing and Spatial Information Sciences* 34 (Part 5): 696–701.

Bosche, F., C. T. Haas, and B. Akinci. 2009. "Automated Recognition of 3D CAD Objects in Site Laser Scans for Project 3D Status Visualization and Performance Control." *Journal of Computing in Civil Engineering* 23 (6): 311–18.

BuildingSmart. 2013. "Industry Foundation Classes Release 4 (IFC4)." http://www.buildingsmart-tech.org/ifc/IFC4/final/html/index.htm.

Conte, Joel P, J Enrique Luco, JI Restrepo, Frieder Seible, and Lelli Van Den Einde. 2004. "UCSD-NEES Large High Performance Outdoor Shake Table." In Proceedings of the 17th ASCE engineering mechanics conference. Newark, DE: University of Delaware.

Dong, L. G., and J. Shan. 2013. “A Comprehensive Review of Earthquake-Induced Building Damage Detection with Remote Sensing Techniques.” *Isprs Journal of Photogrammetry and Remote Sensing* 84 (October): 85–99.

Dong, P. L., and H. D. Guo. 2012. “A Framework for Automated Assessment of Post-Earthquake Building Damage Using Geospatial Data.” *International Journal of Remote Sensing* 33 (1): 81–100.

Eastman, C.M., P. Teicholz, R. Sacks, and K. Liston. 2011. *BIM Handbook: A Guide to Building Information Modeling for Owners, Managers, Architects, Engineers, Contractors, and Fabricators*. Hoboken, NJ: John Wiley and Sons.

EERI. 2014a. “Concrete Buildings Damaged in Earthquakes.” http://db.concretecoalition.org/list.

EERI. 2014b. “Turkey School Bldgs - Moment Frames.” http://db.concretecoalition.org/building/132.

EERI. 2014c. “Ilgi Moble Building.” http://db.concretecoalition.org/building/135.

Eo, Yang Dam, Mu Wook Pyeon, Sun Woong Kim, Jang Ryul Kim, and Dong Yeob Han. 2012. “Coregistration of Terrestrial Lidar Points by Adaptive Scale-Invariant Feature Transformation with Constrained Geometry.” *Automation in Construction* 25 (August): 49–58.

FEMA. 1998. *Evaluation of Earthquake Damaged Concrete and Masonry Wall Buildings: Basic Procedures Manual-FEMA 306*. Federal Emergency Management Agency.

German, S., J. Jeon, Z. Zhu, C. Bearman, I. Brilakis, R. DesRoches, and L. Lowes. 2013. “Machine Vision-Enhanced Postearthquake Inspection.” *Journal of Computing in Civil Engineering* 27 (6): 622–34.

IfcOpenShell. 2014. “IfcOpenShell.” http://ifcopenshell.org/.

Ip, Cheuk Yiu, and Satyandra K. Gupta. 2007. “Retrieving Matching CAD Models by Using Partial 3D Point Clouds.” *Computer-Aided Design and Applications* 4 (5): 629–38.

Kasai, Kazuhiko, Hiroshi Ito, Yoji Ooki, Tsuyoshi Hikino, Koichi Kajiwara, Shojiro Motoyui, Hitoshi Ozaki, and Masato Ishii. 2010. “Full-Scale Shake Table Tests of 5-Story Steel Building with Various Dampers.” In Proc., 7th Intern. Conf. on Urban Earthquake Engin. & 5th Intern. Conf. on Earthquake Engin.

Kashani, A., P. Crawford, S. Biswas, A. Graettinger, and D. Grau. 2014. “Automated Tornado Damage Assessment and Wind Speed Estimation Based on Terrestrial Laser Scanning.” *Journal of Computing in Civil Engineering*, May, 04014051.

Krishnan, Sriram, Christopher Crosby, Viswanath Nandigam, Minh Phan, Charles Cowart, Chaitanya Baru, and Ramon Arrowsmith. 2011. “OpenTopography: A Services Oriented Architecture for Community Access to LIDAR Topography.” In *Proceedings of the 2nd International Conference on Computing for Geospatial Research & Applications*, 7. ACM. http://dl.acm.org/citation.cfm?id=1999327.

LEICA. 2014. “Leica ScanStation C10 - The All-in-One Laser Scanner for Any Application - Leica Geosystems - HDS.” Accessed October 6. http://hds.leica-geosystems.com/en/Leica-ScanStation-C10_79411.htm.

Lichti, D., S. Gordon, and T. Tipdecho. 2005. “Error Models and Propagation in Directly Georeferenced Terrestrial Laser Scanner Networks.” *Journal of Surveying Engineering* 131 (4): 135–42.

Liu, W., P. L. Dong, J. B. Liu, and H. D. Guo. 2013. “Evaluation of Three-Dimensional Shape Signatures for Automated Assessment of Post-Earthquake Building Damage.” *Earthquake Spectra* 29 (3): 897–910.

Ma, L, R Sacks, and R Zeibak-Shini. 2014. “Information Modeling of Earthquake-Damaged Reinforced Concrete Structures.” *Advanced Engineering Informatics*.

Ohtani, Keiichi, Nobuyuki Ogawa, Tsuneo Katayama, and Heki Shibata. 2003. “Construction of E-Defense (3-D Full-Scale Earthquake Testing Facility).” In Proc. of Second International Symposium on New Technologies for Urban Safety of Mega Cities in Asia, 69–76.

Open CASCADE. 2014. “Open CASCADE Technology, 3D Modeling & Numerical Simulation.” http://www.opencascade.org/.

Panagiotou, Marios, José I Restrepo, and Joel P Conte. 2010. “Shake-Table Test of a Full-Scale 7-Story Building Slice. Phase I: Rectangular Wall.” *Journal of Structural Engineering* 137 (6): 691–704.

PNPOLY. 2014. “PNPOLY - Point Inclusion in Polygon Test - WR Franklin (WRF).” http://www.ecse.rpi.edu/Homepages/wrf/Research/Short_Notes/pnpoly.html#3D%2520Polygons.

Previtali, M., L. Barazzetti, R. Brumana, and M. Scaioni. 2014. “Laser Scan Registration Using Planar Features.” *International Archives of the Photogrammetry, Remote Sensing & Spatial Information Sciences* 45.

Pu, Shi, and George Vosselman. 2007. “Extracting Windows from Terrestrial Laser Scanning.” *Intl Archives of Photogrammetry, Remote Sensing and Spatial Information Sciences* 36: 12–14.

Schwarz, S., A. Hanaor, and D. Yankelevsky. 2008. *Horizontal Load Resistance RC Frames with Masonary Infill Panels*. National Building Research Institute, Technion.

Sun, Xianfang, Paul L. Rosin, Ralph R. Martin, and Frank C. Langbein. 2008. “Noise in 3D Laser Range Scanner Data.” In *Shape Modeling and Applications, 2008. SMI 2008. IEEE International Conference on*, 37–45.

Tiedemann, Herbert. 1992. *Earthquakes and Volcanic Eruptions: A Handbook on Risk Assessment*. Swiss Re.

Torok, M., M. Golparvar-Fard, and K. Kochersberger. 2014. “Image-Based Automated 3D Crack Detection for Post-Disaster Building Assessment.” *Journal of Computing in Civil Engineering* 28 (5).

Van de Lindt, John W, Shiling Pei, Steven E Pryor, H Shimizu, and H Isoda. 2010.

"Experimental Seismic Response of a Full-Scale Six-Story Light-Frame Wood Building." *Journal of Structural Engineering* 136 (10): 1262–72.

Zeibak-Shini, R, R Sacks, and S Filin. 2012. "Toward Generation of a Building Information Model of a Deformed Structure Using Laser Scanning Technology." In *14th International Conference on Computing in Civil and Building Engineering (ICCCBE)*. Moscow, Russia.

Zhang, C. Y., and D. Arditi. 2013. "Automated Progress Control Using Laser Scanning Technology." *Automation in Construction* 36 (December): 108–16.

Fig 1(a)
Click here to download high resolution image

Fig 1(b)
Click here to download high resolution image

Fig 2(a)

Click here to download high resolution image

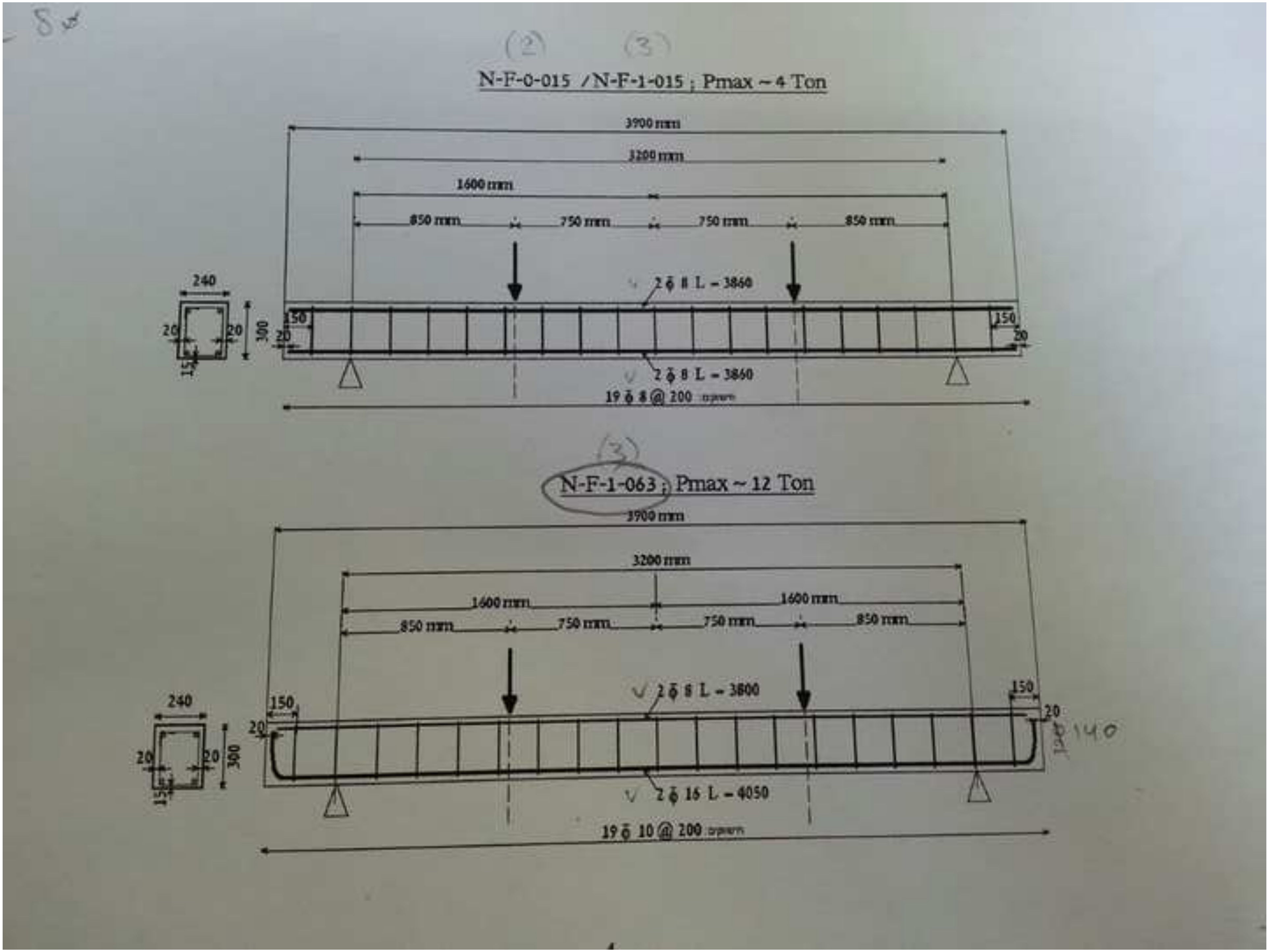

Fig 2(b)

Click here to download high resolution image

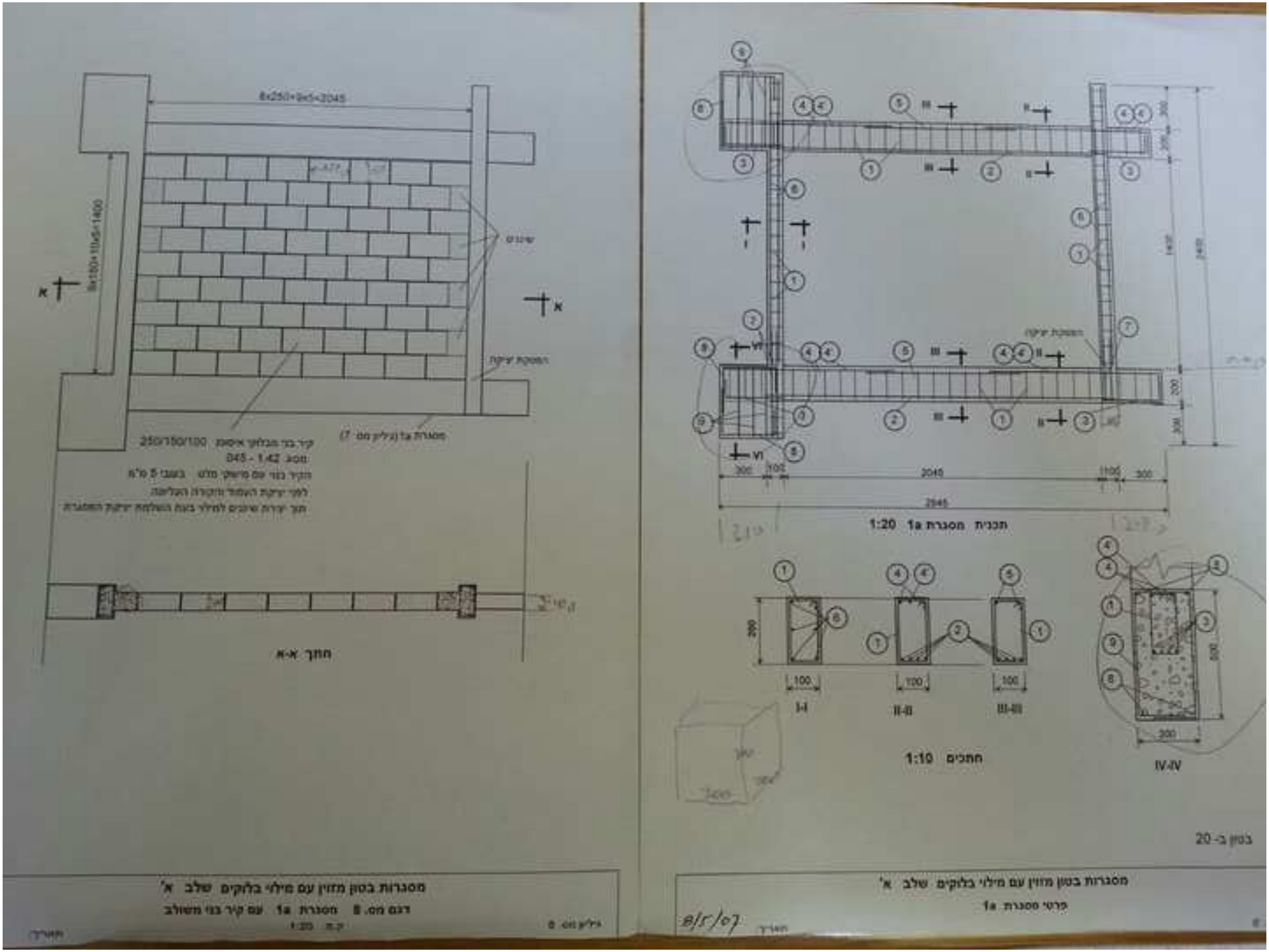

Fig 2(c)

Click here to download high resolution image

Fig 2(d)
Click here to download high resolution image

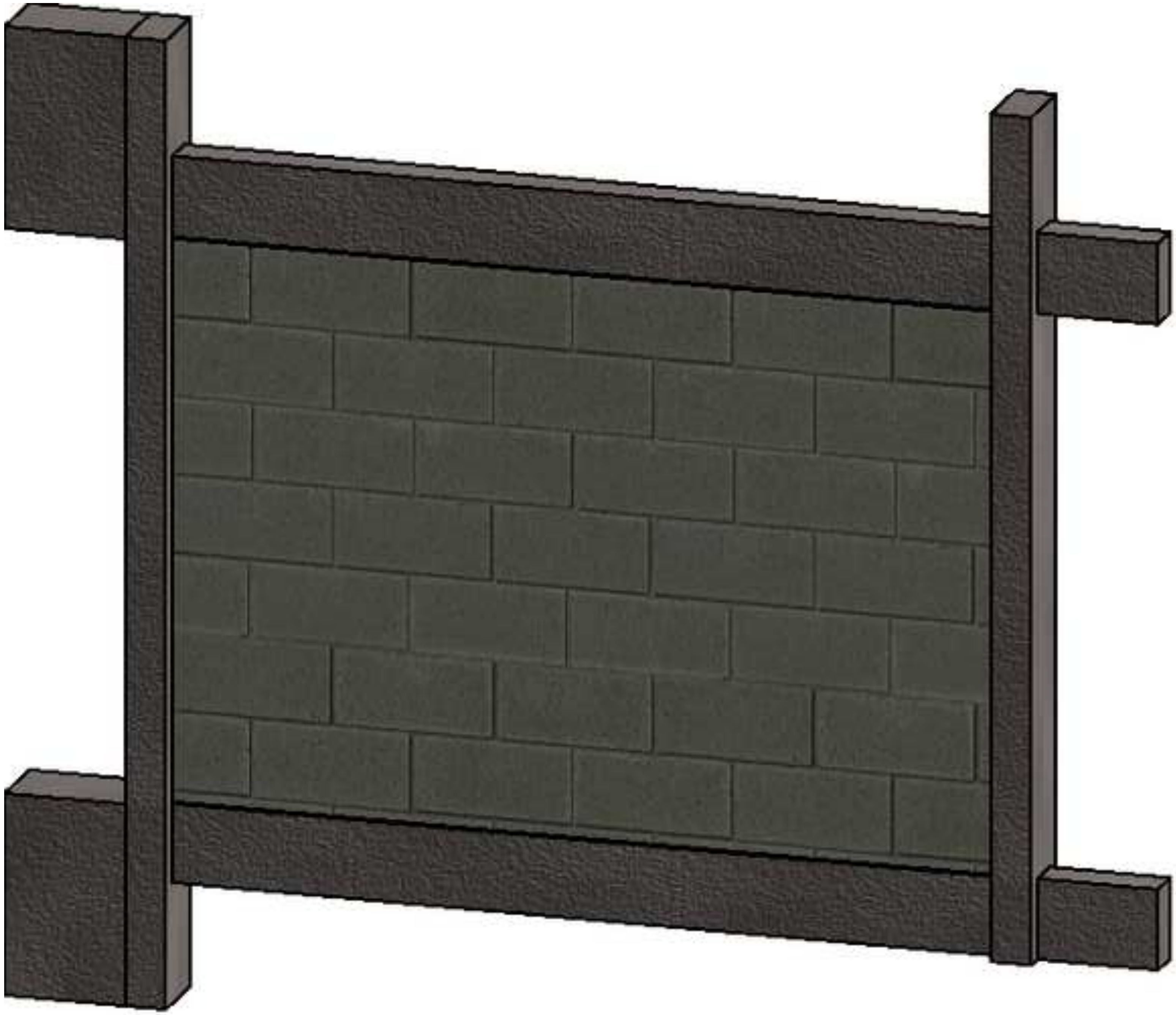

Fig 3(a)
Click here to download high resolution image

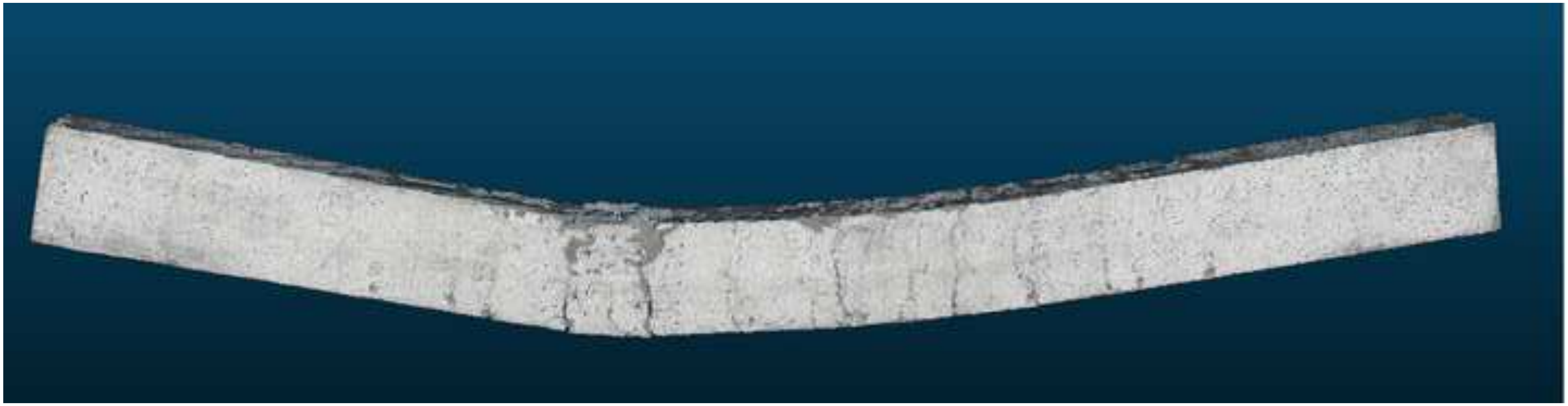

Fig 3(b)
Click here to download high resolution image

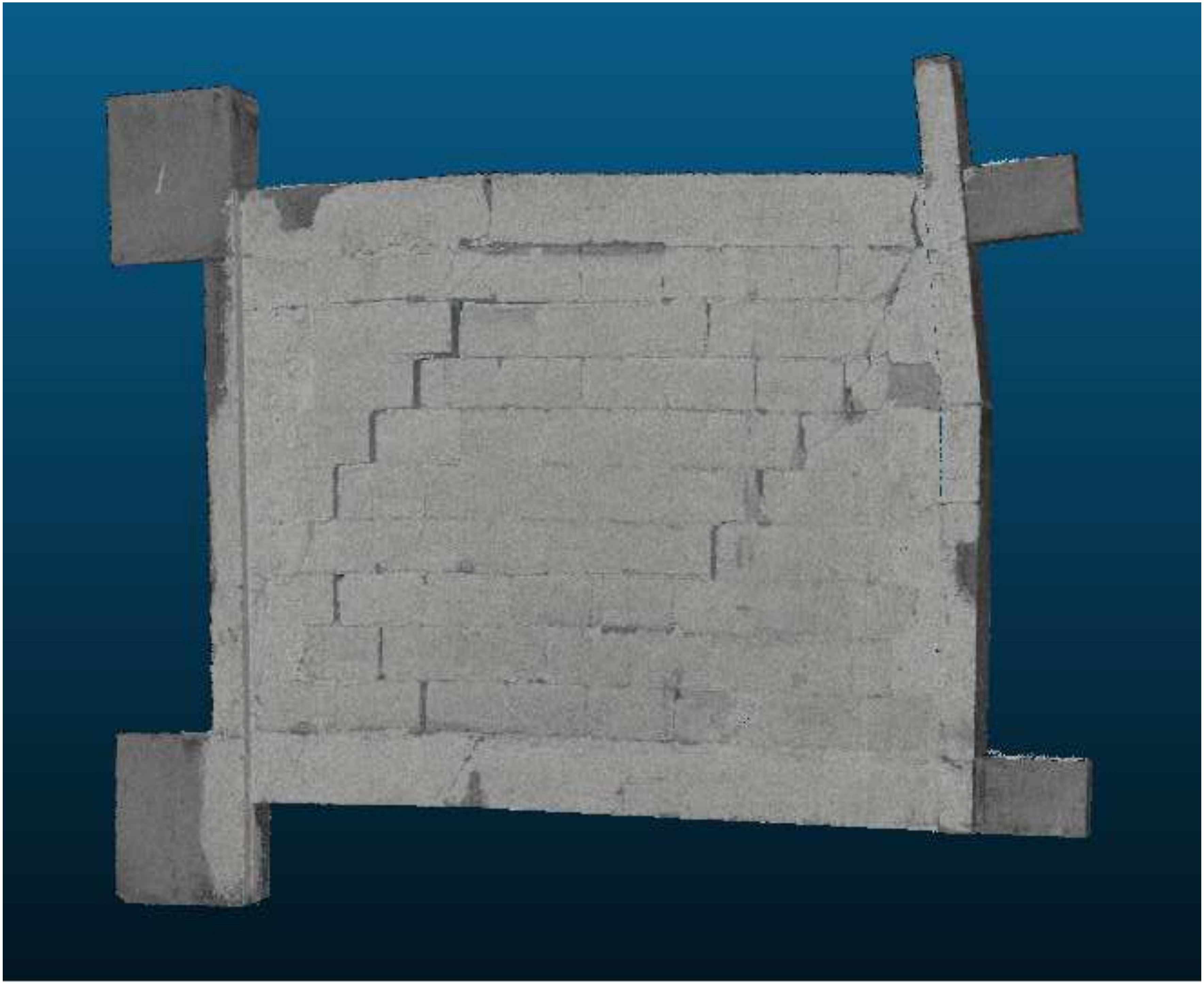

Fig 4
Click here to download high resolution image

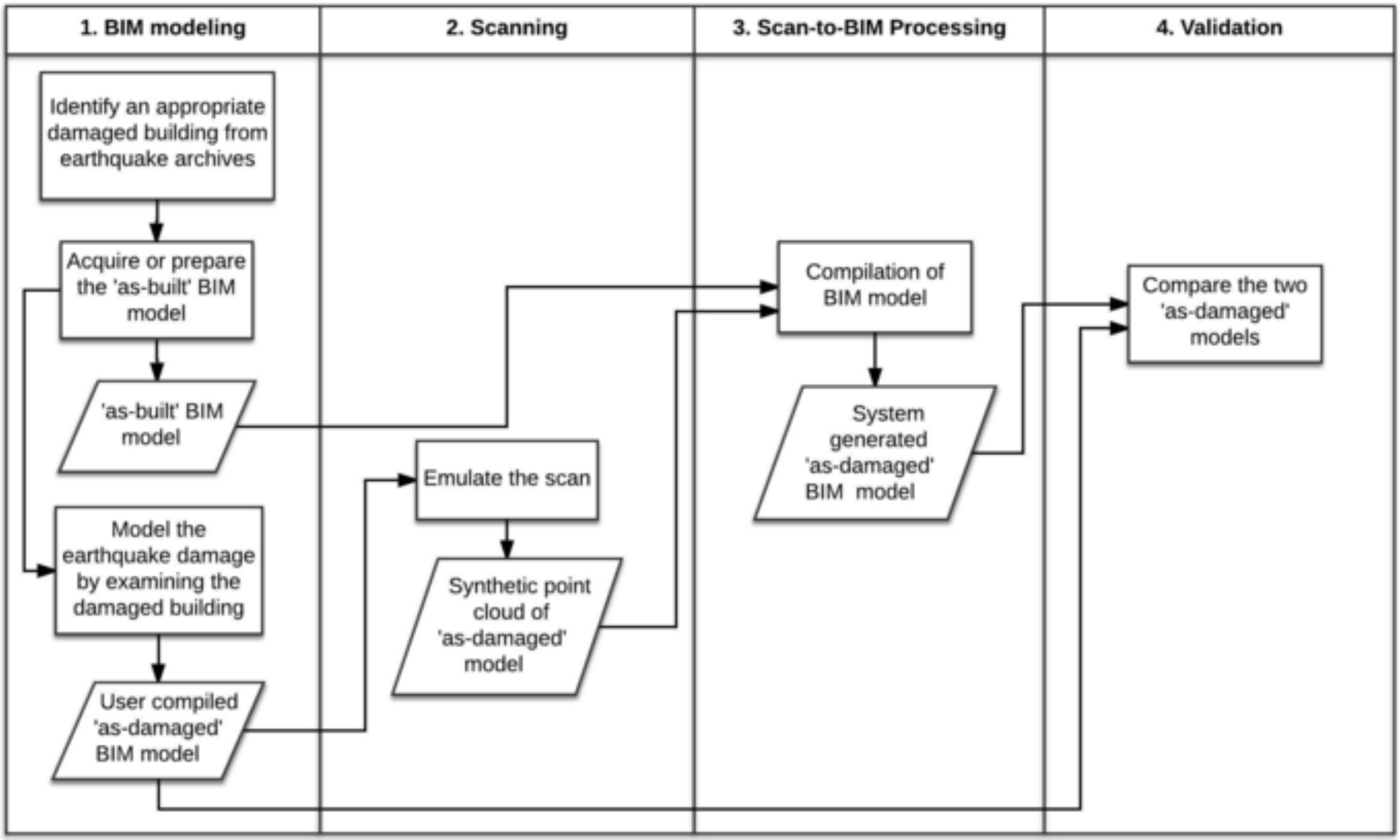

Fig 5
Click here to download high resolution image

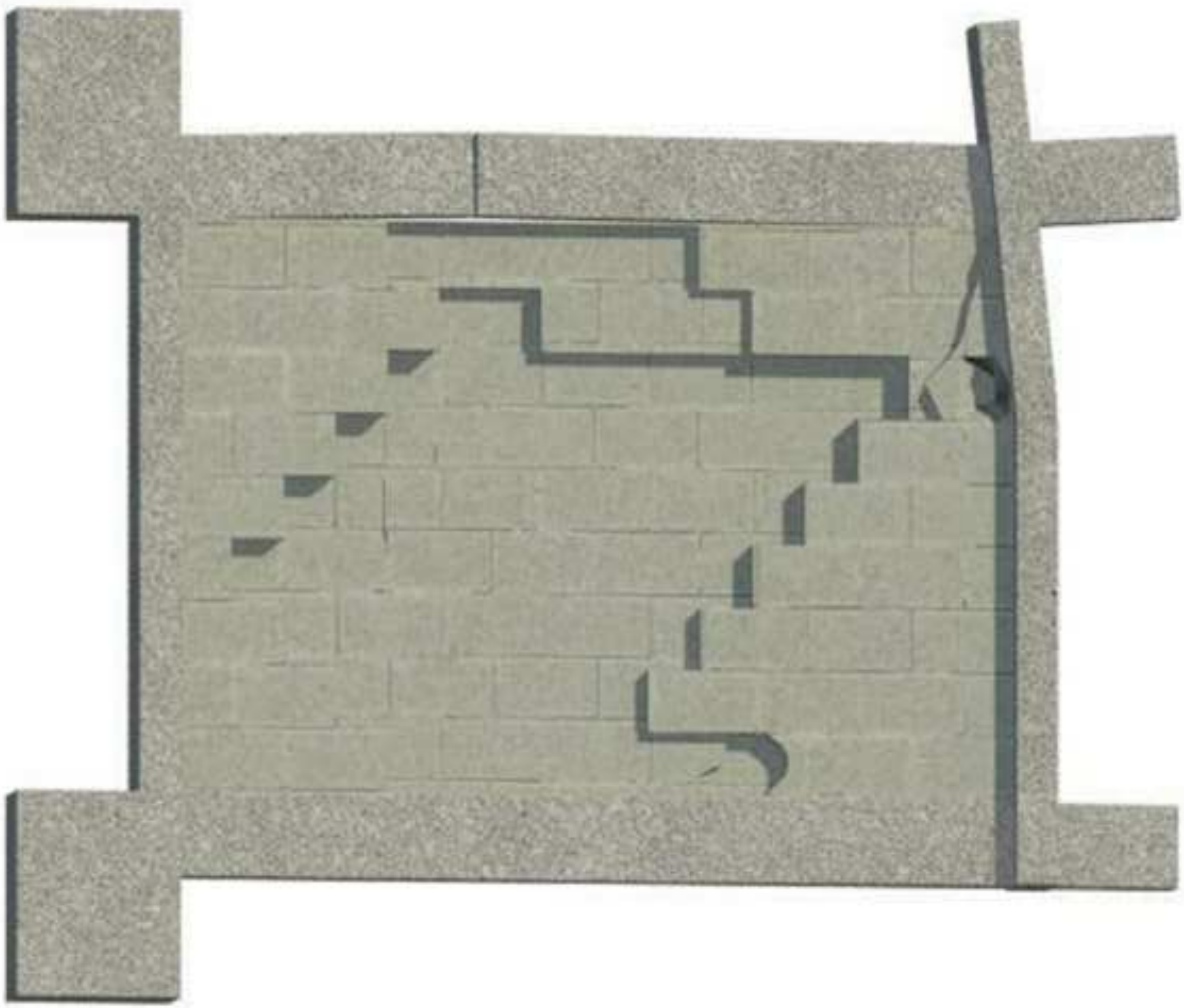

Fig 6

Click here to download high resolution image

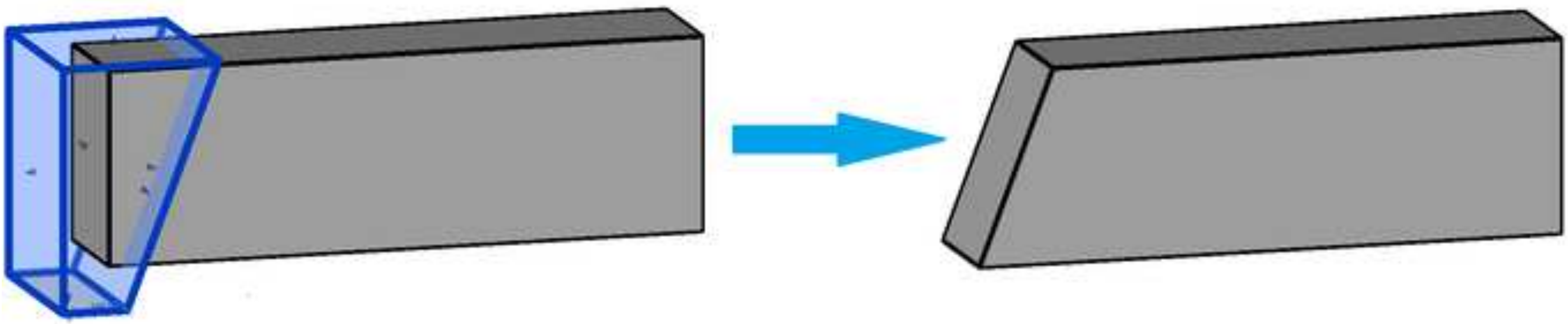

Fig 7(a)
Click here to download high resolution image

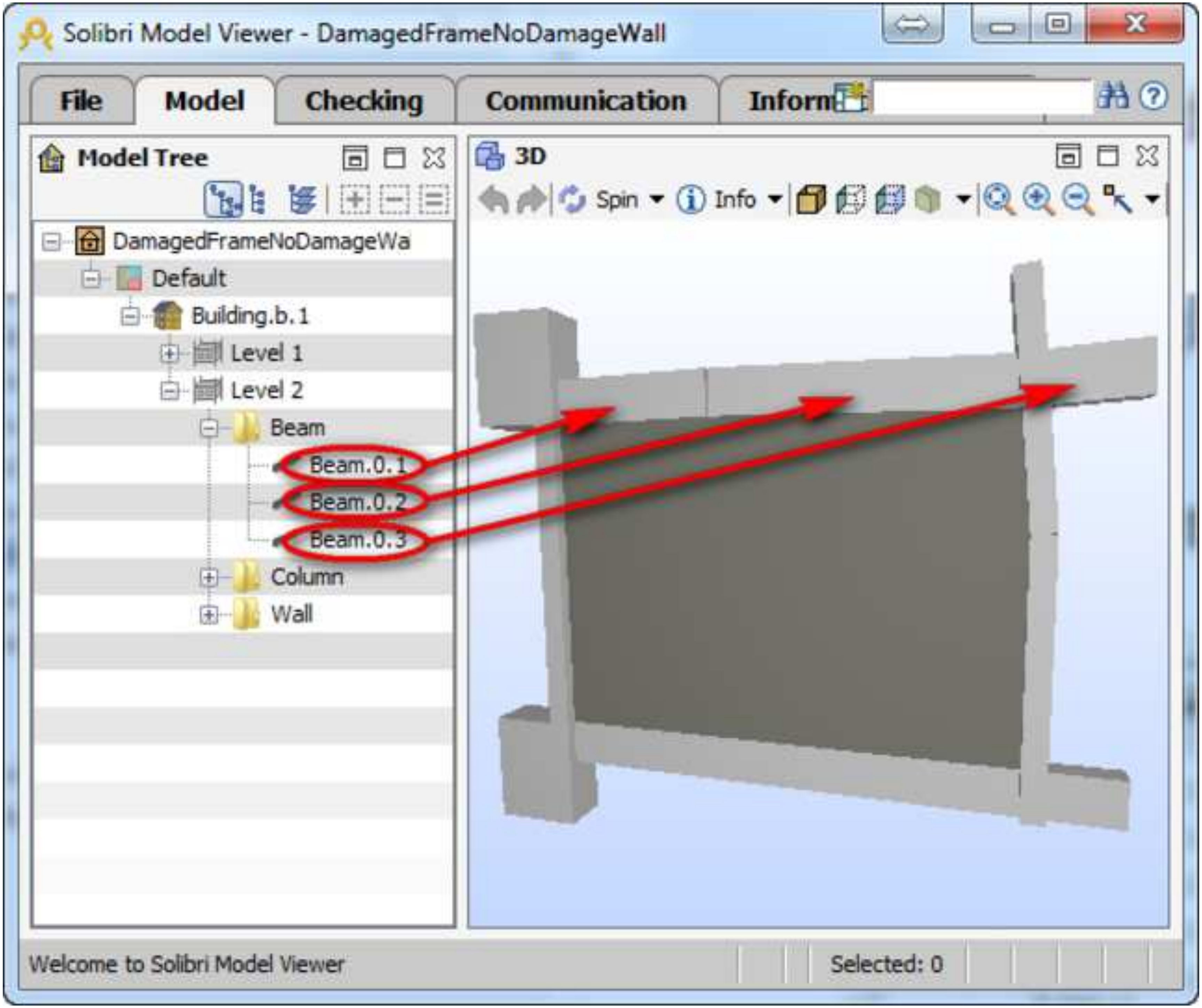

Fig 7(b)
Click here to download high resolution image

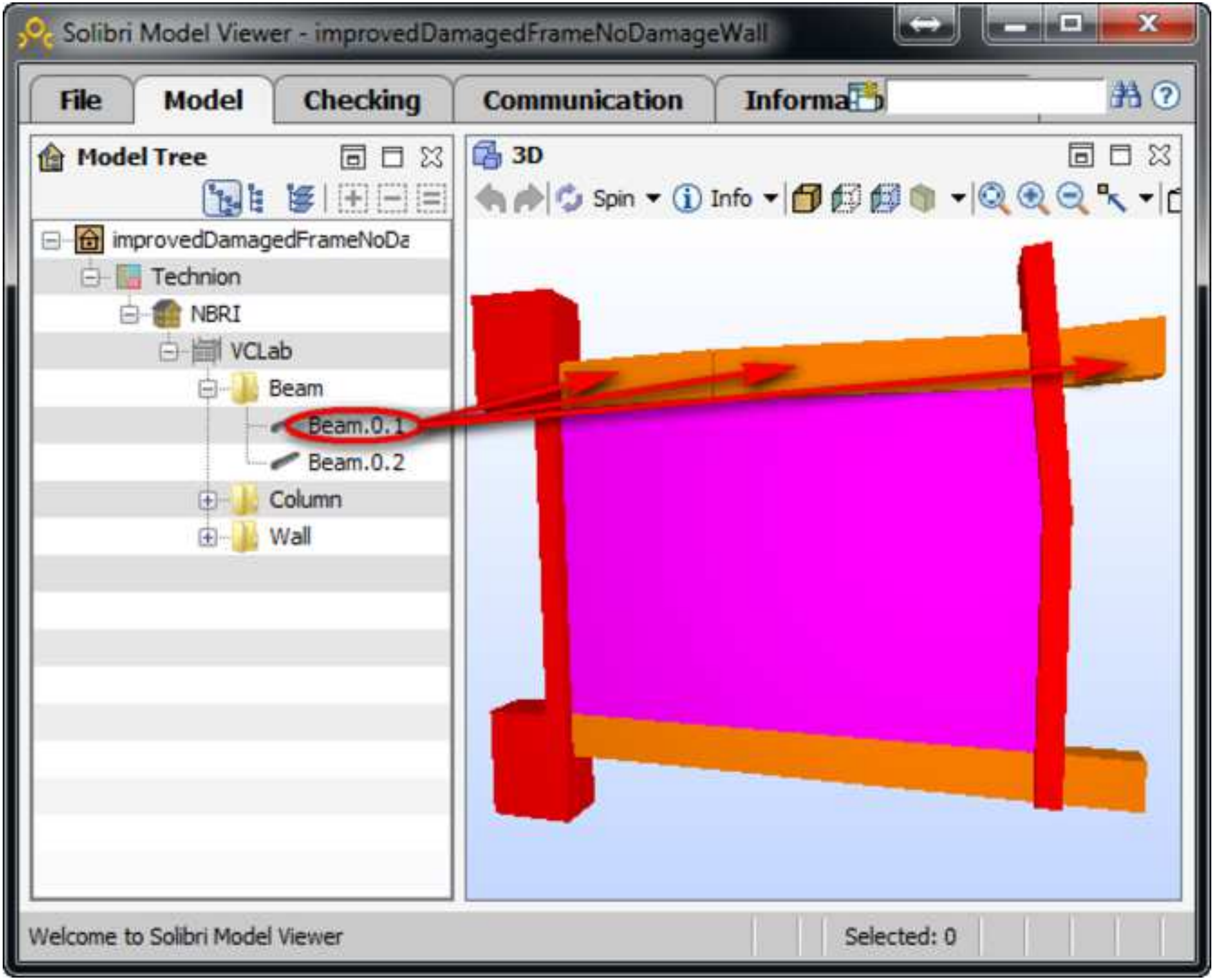

Fig 8
Click here to download high resolution image

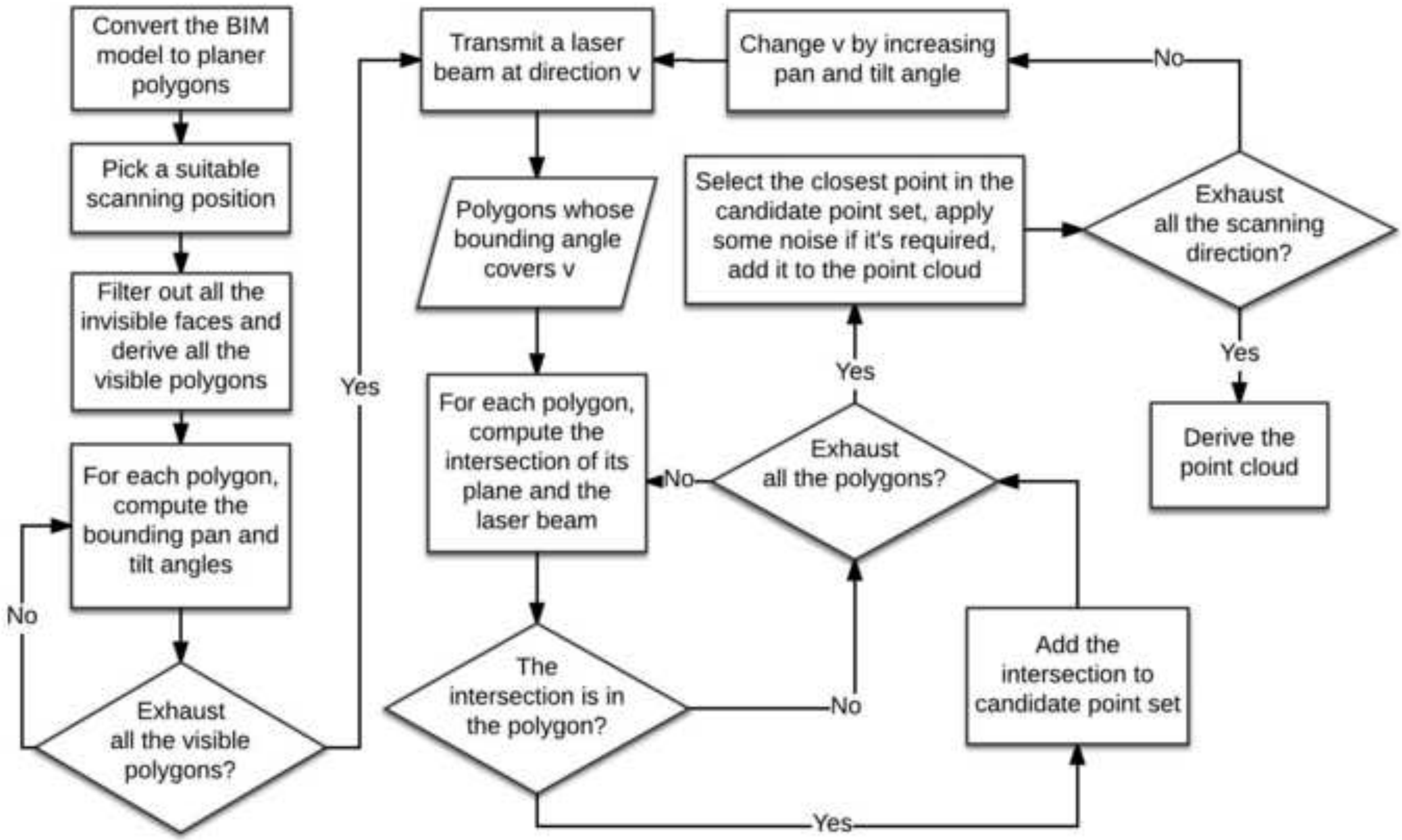

Fig 9
Click here to download high resolution image

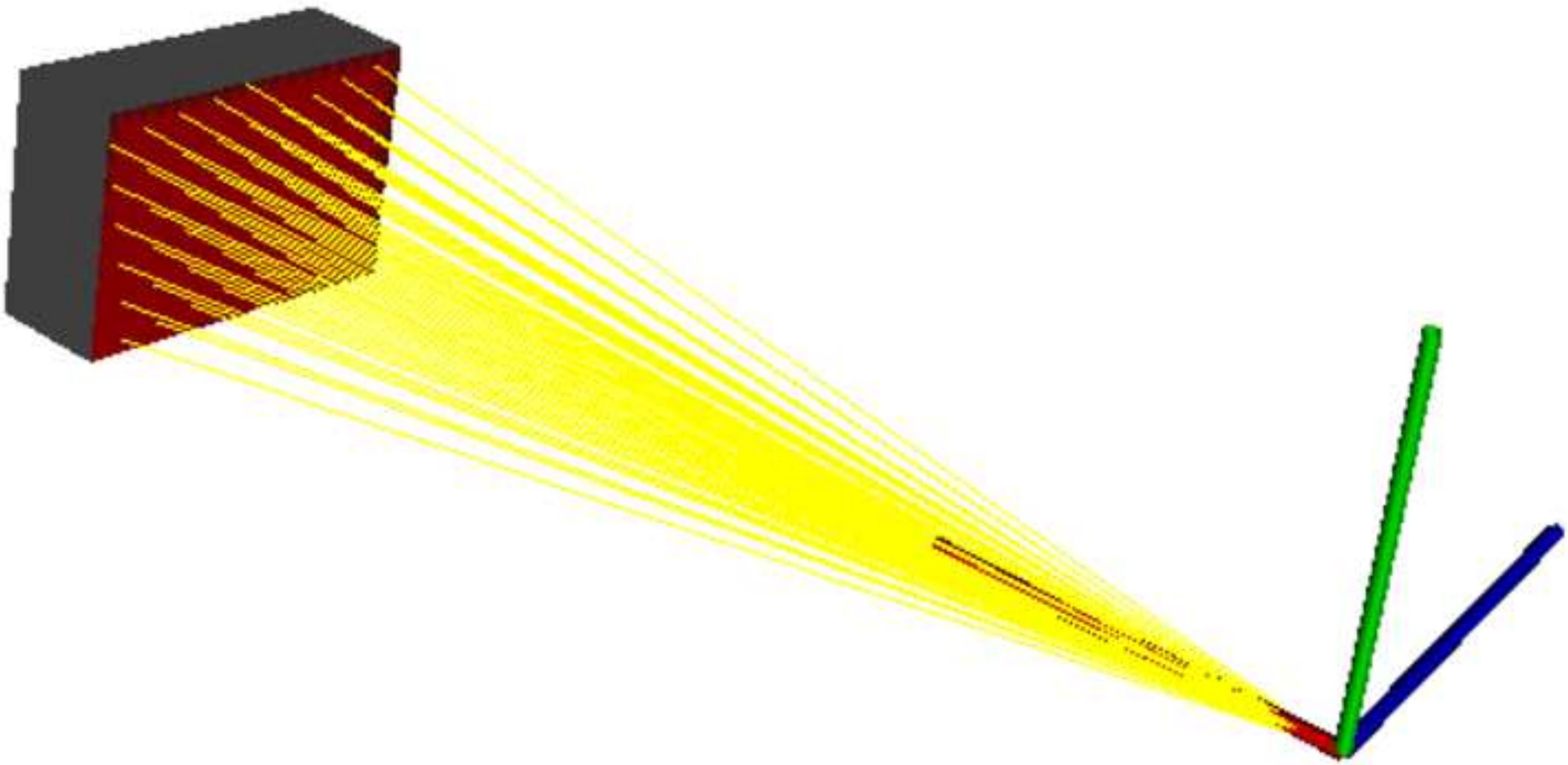

Fig 10
Click here to download high resolution image

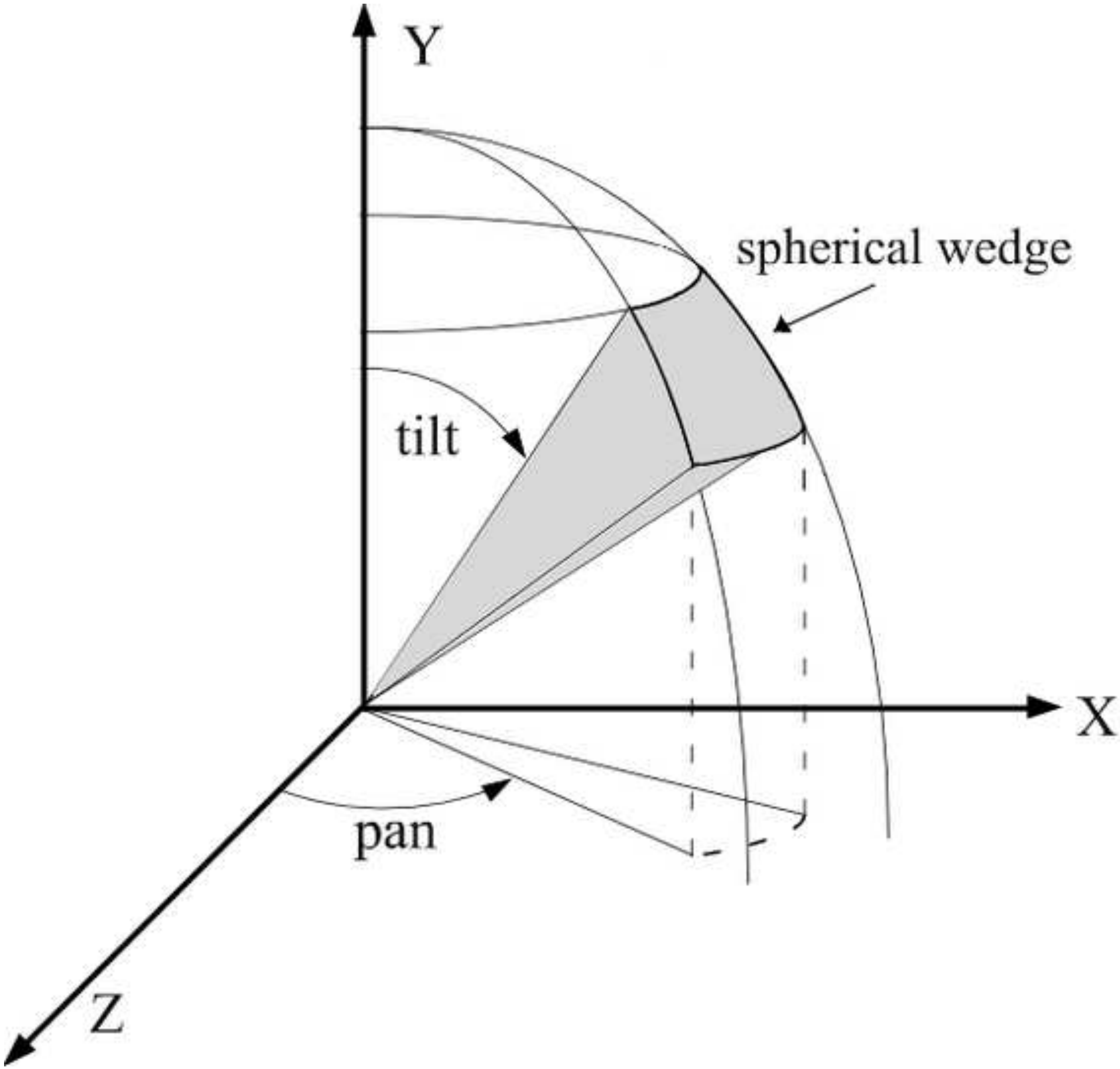

Fig 11(a)

Fig 11(b)

Click here to download high resolution image

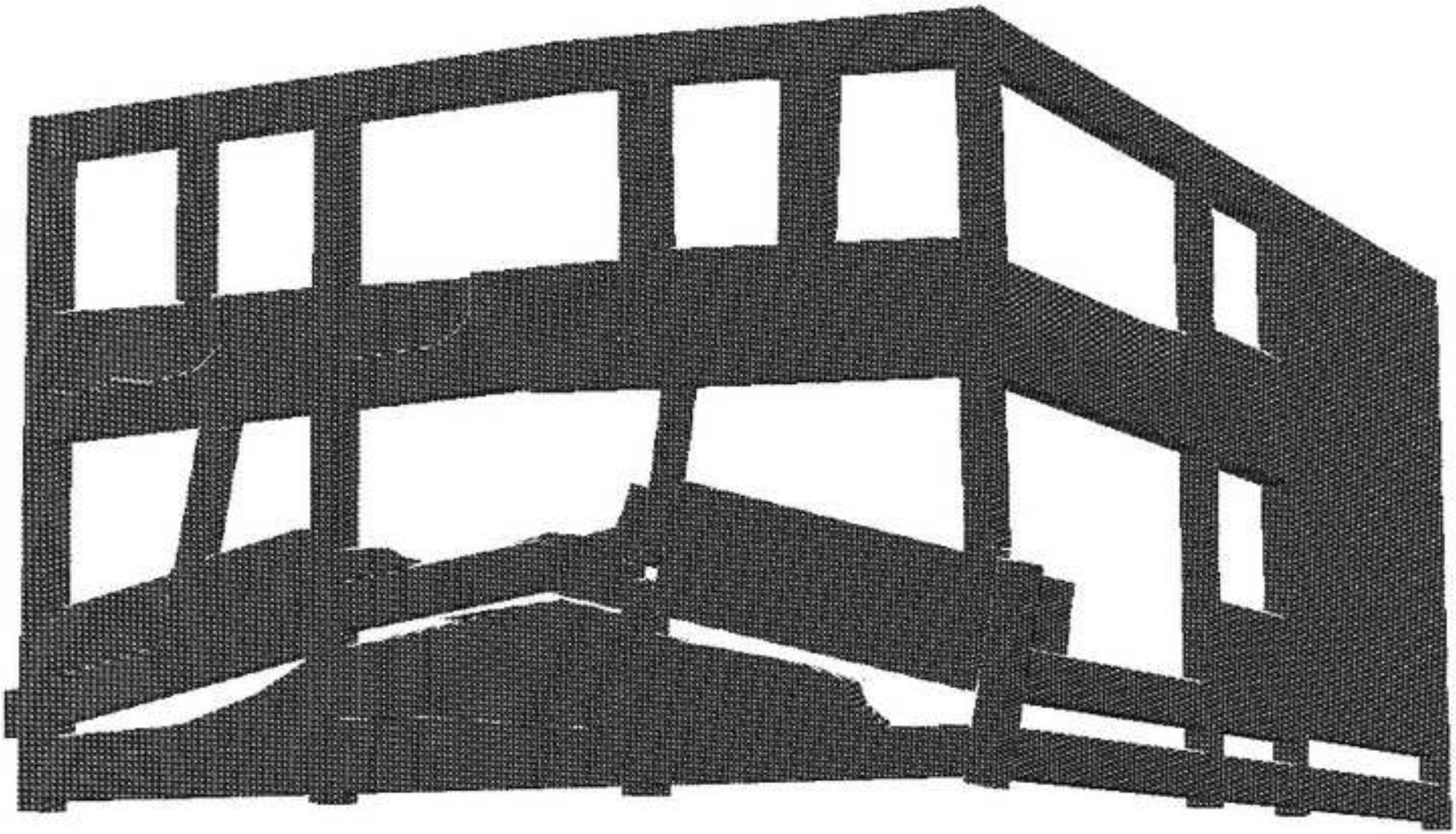

Fig 11(c)
Click here to download high resolution image

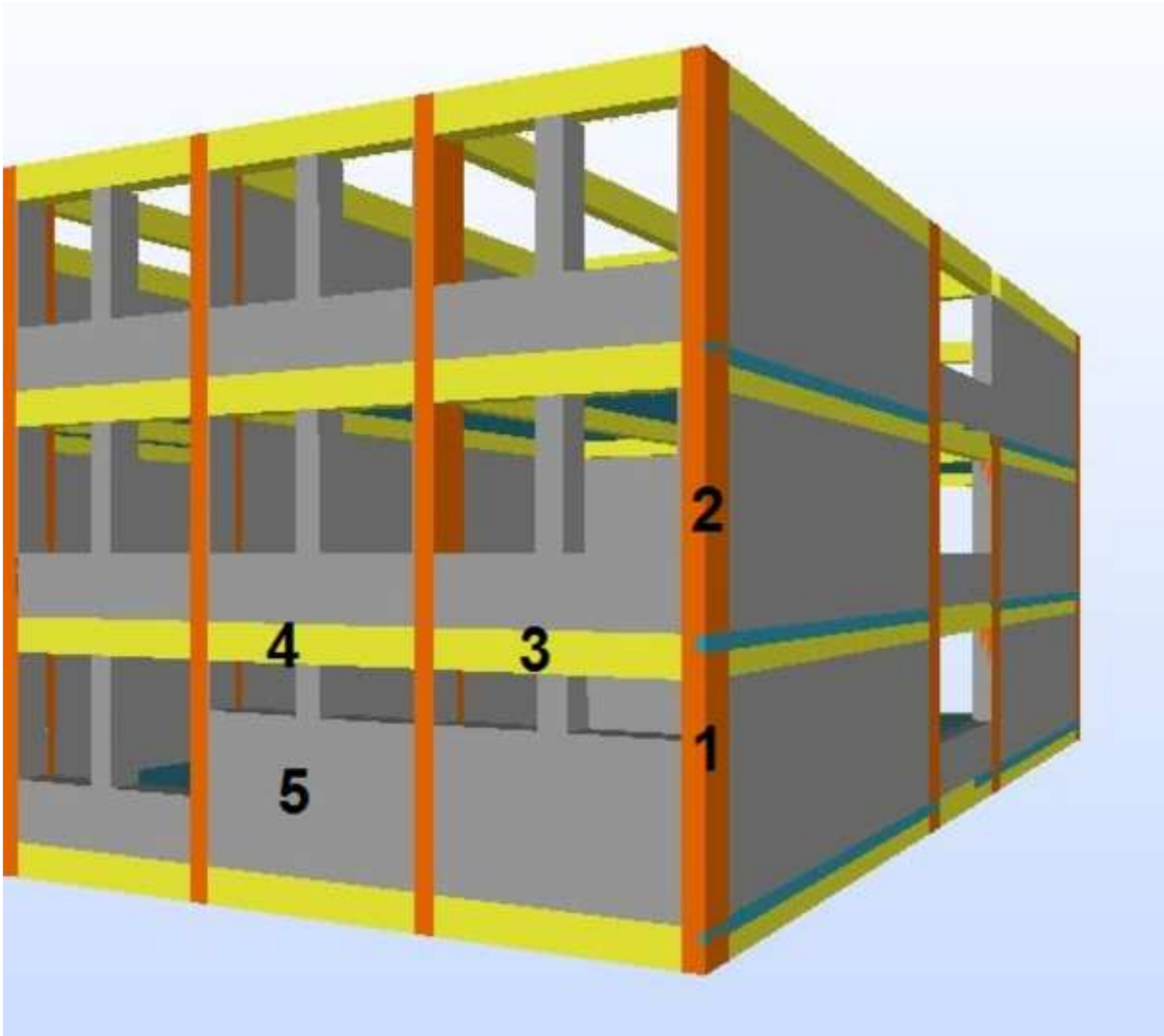

Fig 11(d)
Click here to download high resolution image

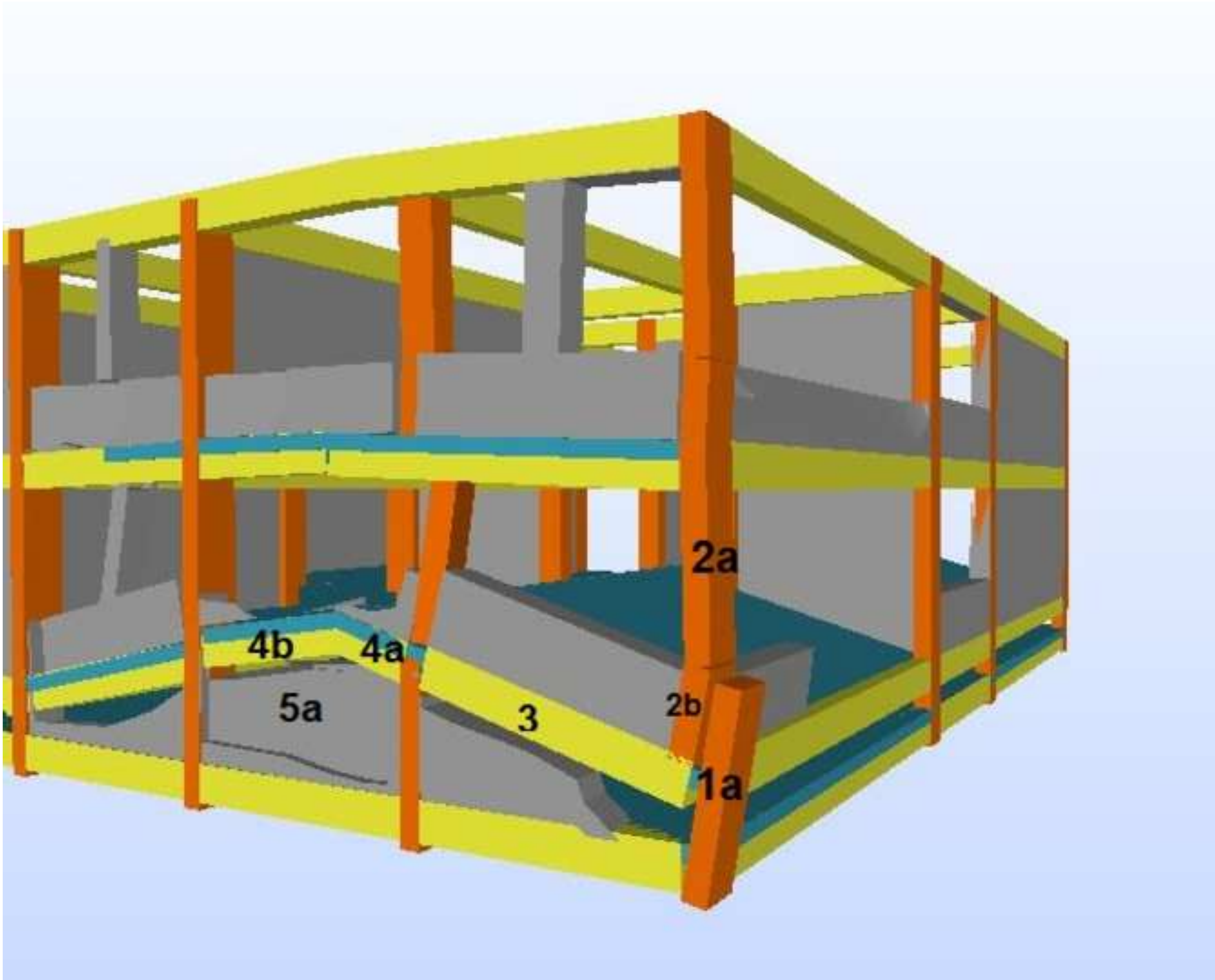

Fig 12(a)
Click here to download high resolution image

Fig 12(b)
Click here to download high resolution image

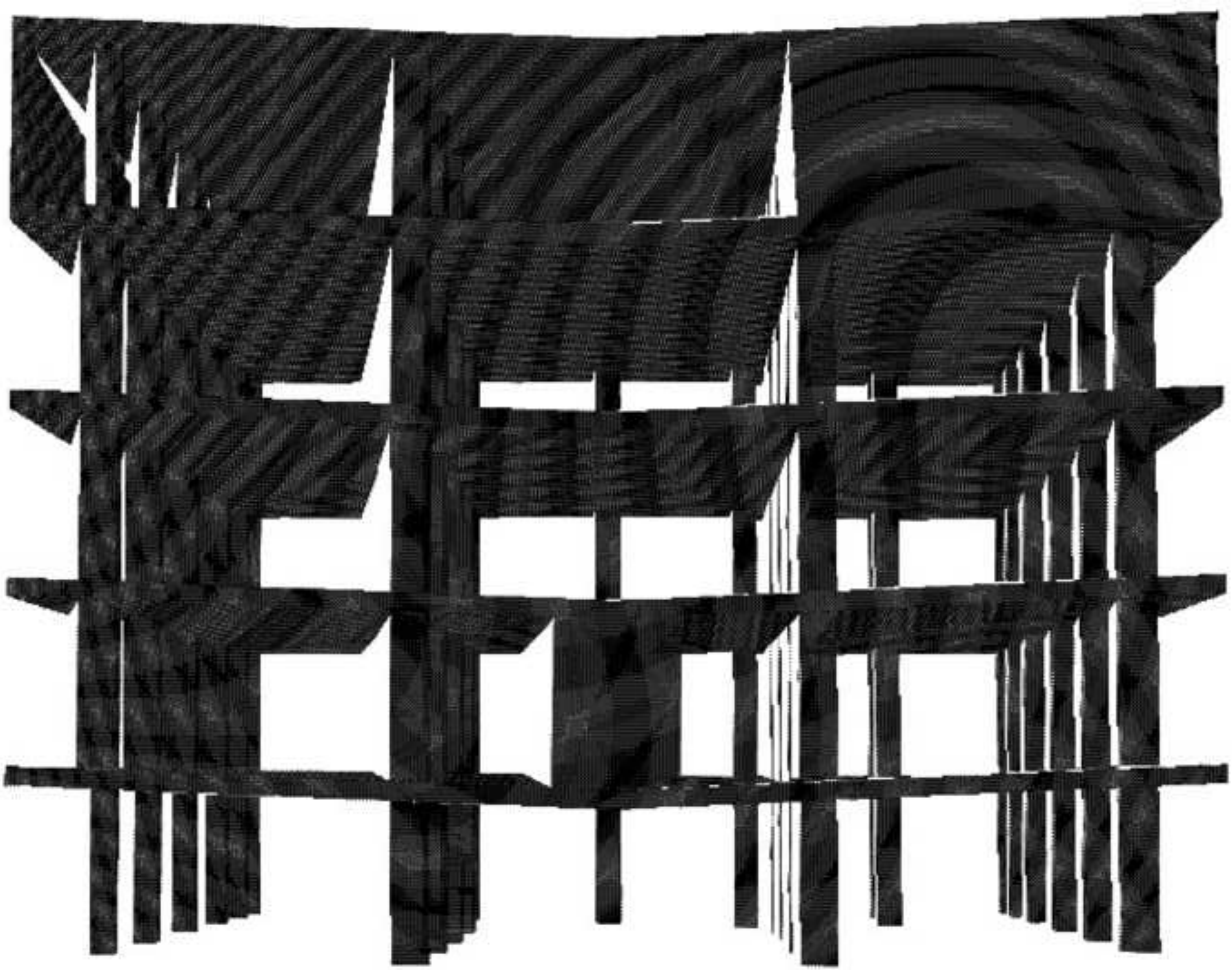

Fig 12(c)

Click here to download high resolution image

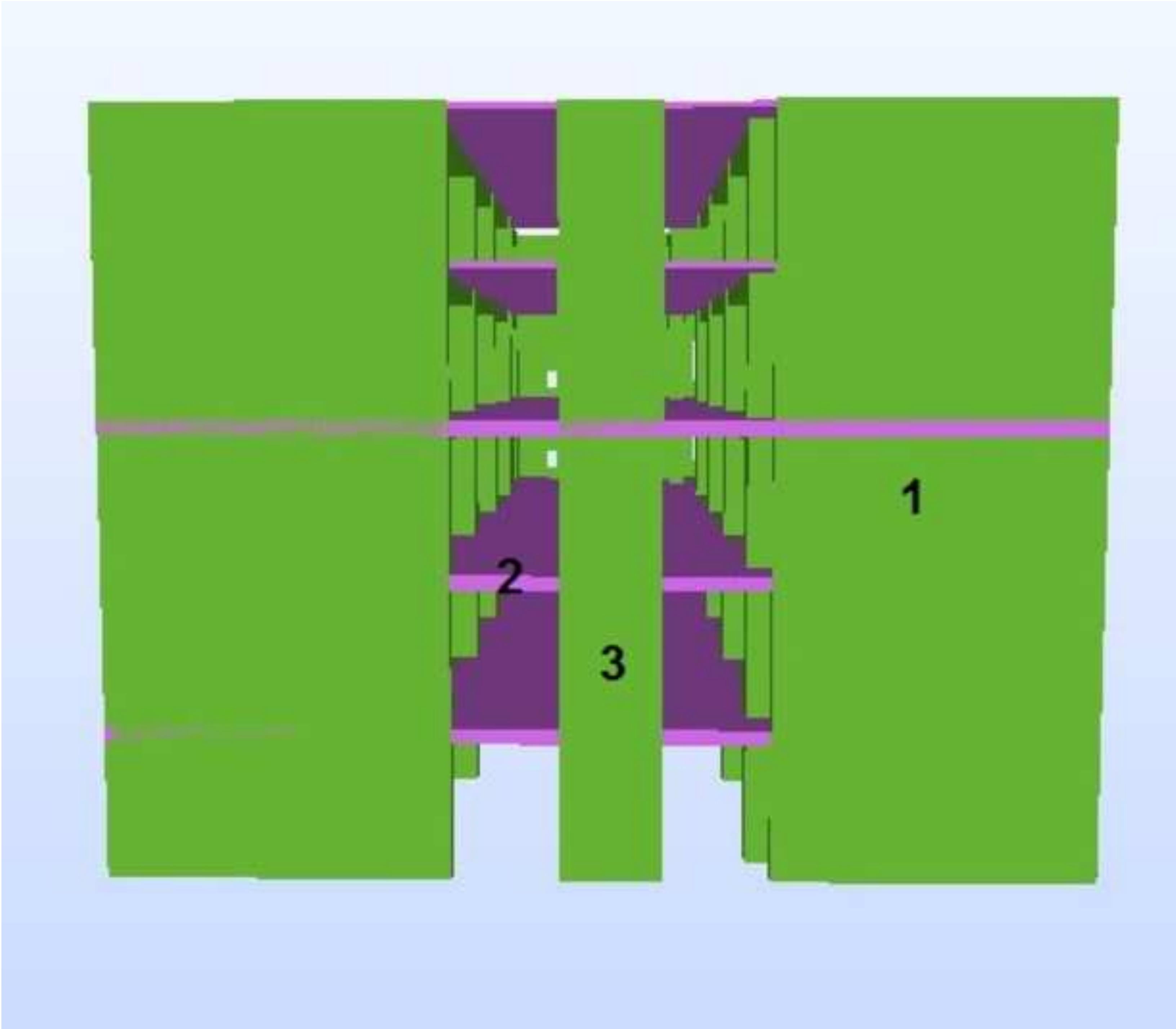

Fig 12(d)
Click here to download high resolution image

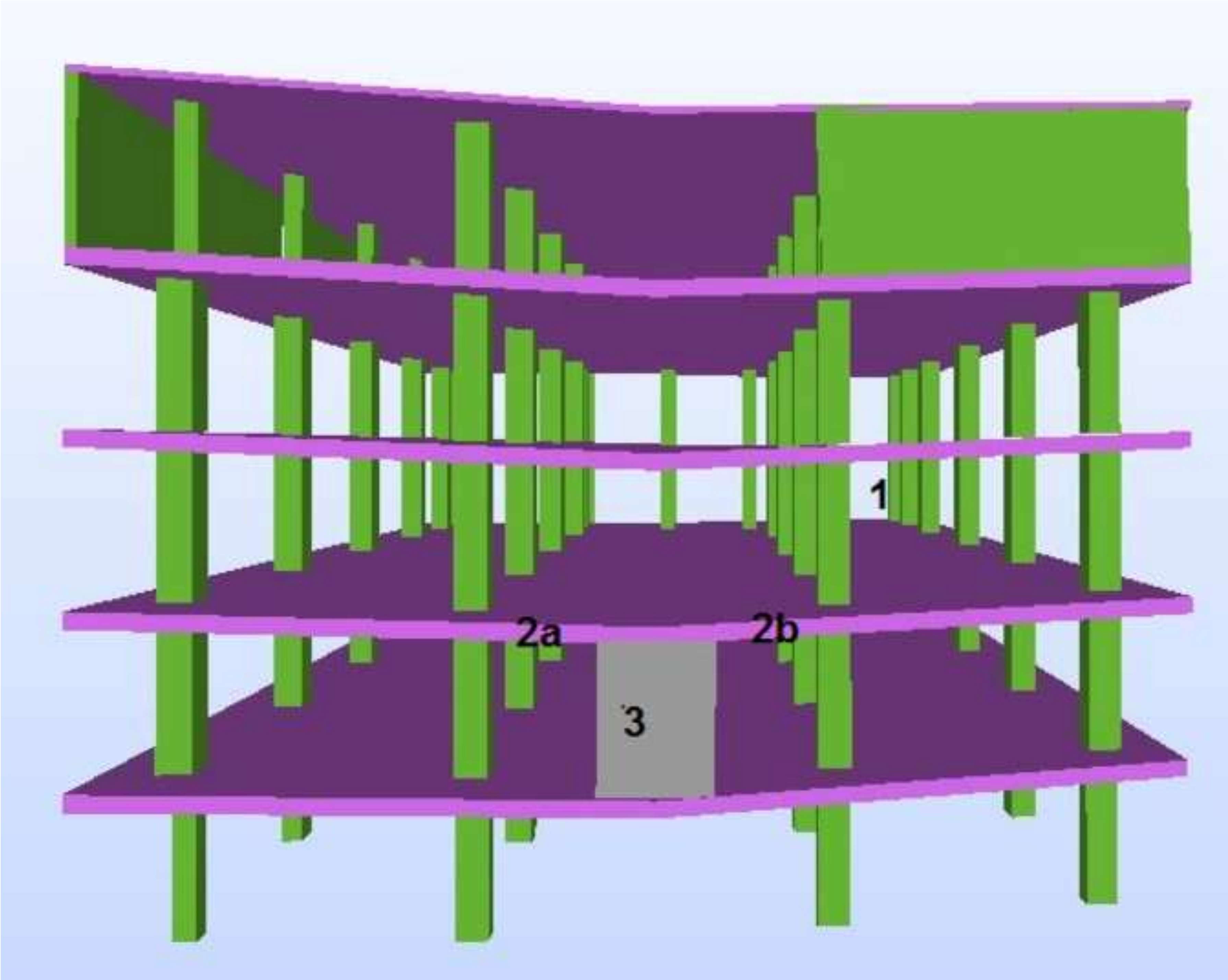

Fig 13(a)
Click here to download high resolution image

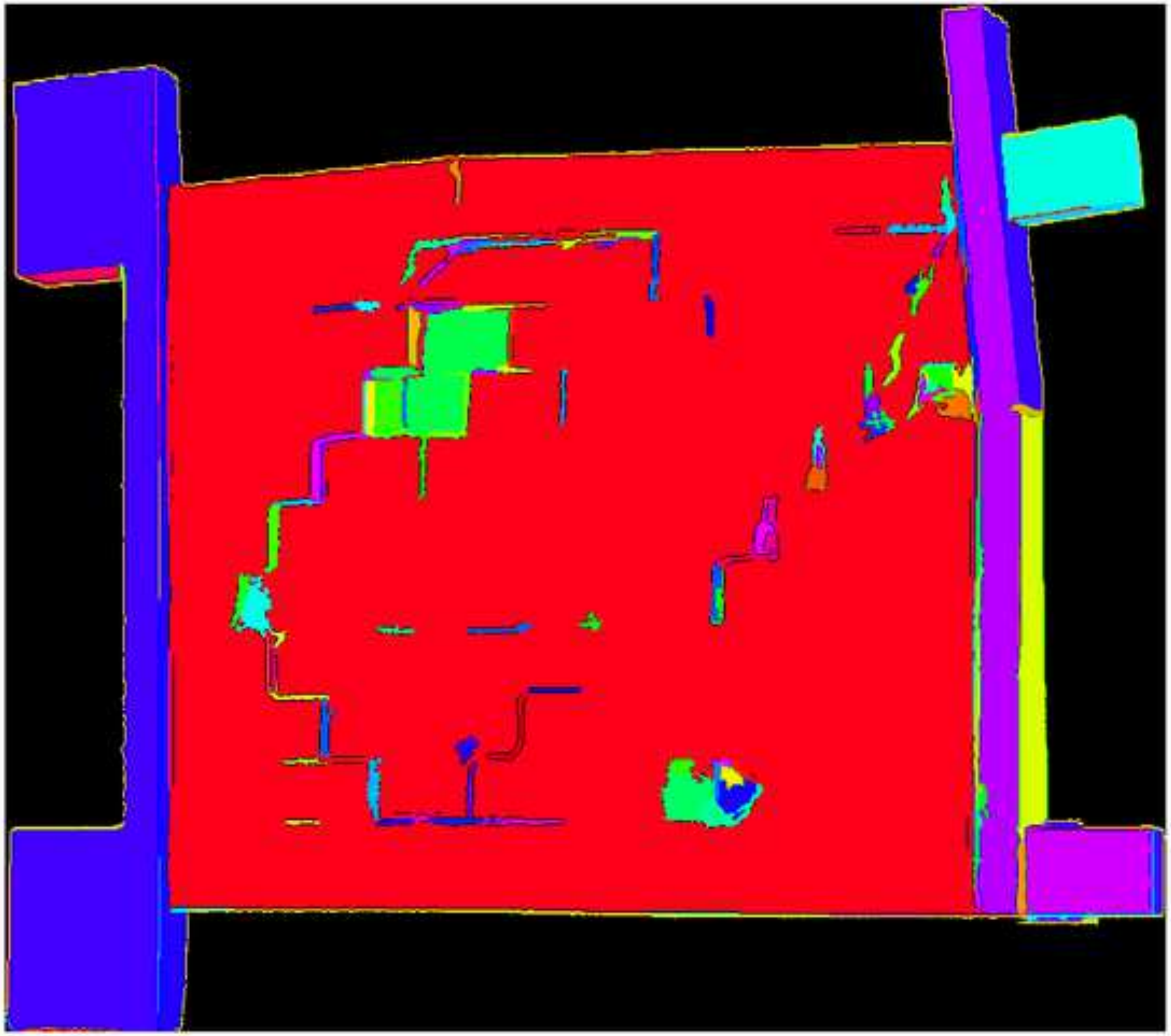

Fig 13(b)
Click here to download high resolution image

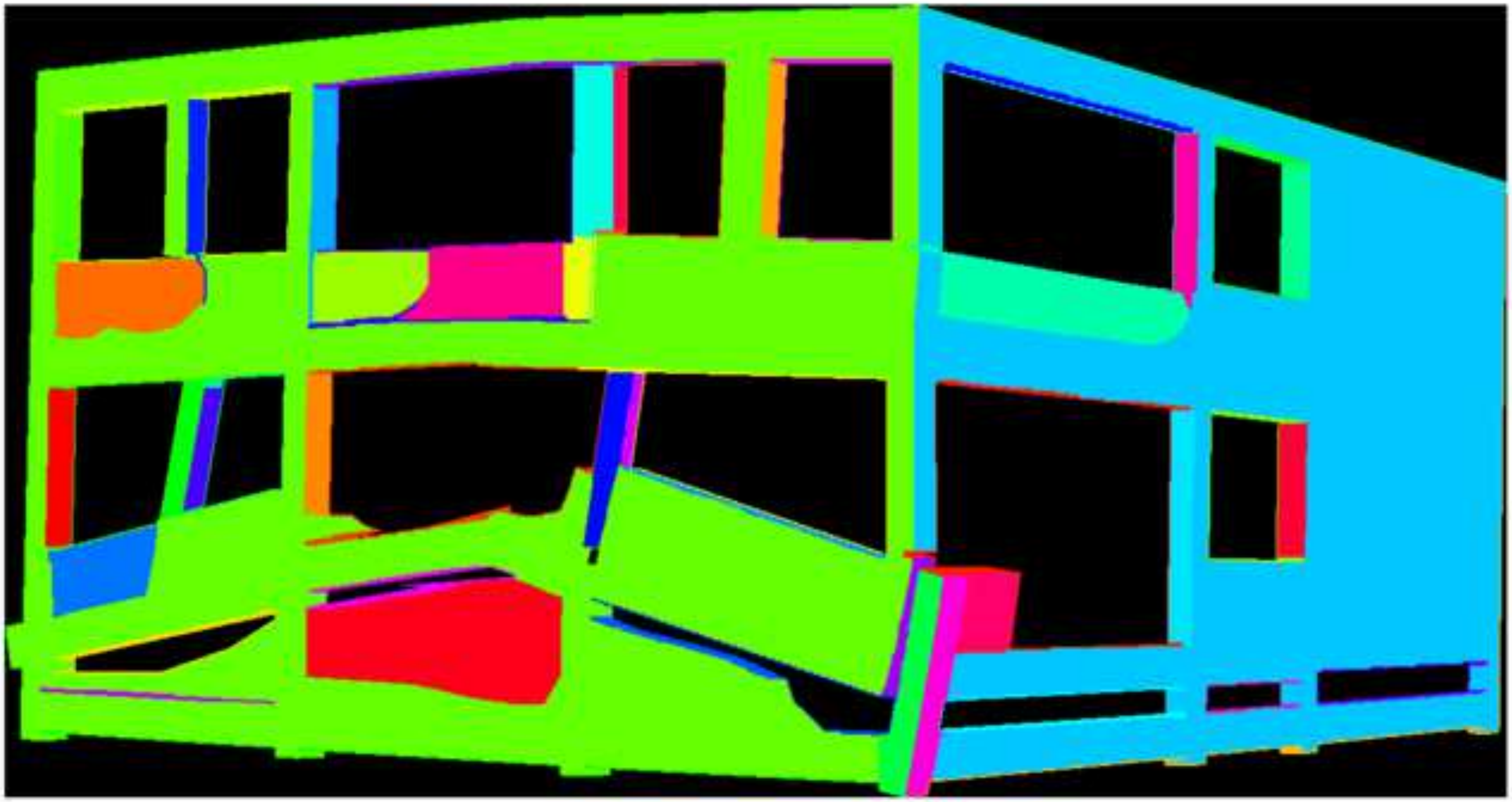

Fig. 1. Reinforced concrete specimens tested at NBRI: (a) a damaged reinforced concrete beam and (b) a damaged reinforced concrete frame wall with autoclaved cement block infill.

Fig. 2. Preparation of as-built BIM model: (a) 2D drawing of the reinforced concrete beam; (b) 2D drawings of the reinforced concrete frame; (c) 'As-built' BIM model of the beam; (d) 'As-built' BIM model of the frame

Fig. 3. Point cloud of (a) the beam and (b) the wall frame.

Fig. 4. BIM Modeling and Scan emulation steps (1 and 2) within the context of the broad earthquake 'Scan-to-BIM' research process

Fig. 5. Modeling of damaged building components in BIM tools

Fig. 6. The ‘as-damaged’ frame modeled in Revit.

Fig. 7. Enrichment of the 'as-damaged' model: (a)'As-damaged' model built in Revit; (b)Aggregated geometry resulting from the custom-built post-processor

Fig. 8. Workflow of the laser scanning emulator

Fig. 9. The emulator "transmits" a laser beam

Fig. 10. Pan and tilt angle boundary

Fig. 11. Preparation of the 'as-damaged' model for the damaged school: (a) Photograph showing earthquake damage to the school (EERI 2014b); (b) synthetic point clouds of the external facades of the damaged school; (c) as-built model of the school; (d) 'as-damaged' model of the school

Fig. 12. Preparation of the 'as-damaged' model for the residential building: (a) Photograph showing earthquake damage to the building (EERI 2014c); (b) synthetic

point clouds of the external facades of the building; (c) 'as-built' model of the building; (d) 'as-damaged' model of the building

Fig. 13. Segmentation results of (a) the physical specimen and (b) the synthetic